

PERFORMANCE ANALYSIS OF  
ADAPTIVE BLIND EQUALIZATION ALGORITHMS FOR NOISY FIR AND IIR  
CHANNELS

By

AWWAB QASIM ALTHAHAB

B.S., University of Babylon, Iraq, 2007

A thesis submitted to the  
Faculty of the Graduate School of the  
University of Colorado at Denver in partial fulfillment  
of the requirements for the degree of  
Master of Science  
Electrical Engineering

2013

This thesis for the Master of Science degree by

Awwab Qasim Althahab

has been approved for the

Electrical Engineering Degree

by

Miloje Radenkovic, Chair

Yiming Deng

Tim Lei

02 / 21 / 2013

Althahab, Awwab Qasim (M.S., Electrical Engineering)

## Performance Analysis of Adaptive Blind Equalization Algorithms for Noisy FIR and IIR Channels

Thesis directed by Professor Miloje Radenkovic

### **ABSTRACT**

This thesis addresses the problem of blind adaptive equalization of finite impulse response (FIR) and infinite impulse response (IIR) channels (their characteristics are unknown) in the fractionally sampling scenario. An adaptive equalizer is used at the receiver to compensate the time dispersion induced by noisy communication channels and eliminate the effect of Inter-Symbol-Interference (ISI). In other words, the overall our system model, which is a cascade connection of the channel and equalizer, provides nearly an ideal transmission medium that the information source signals can be sent through. Due to this and rely only on probabilistic and statistical properties (Second Order Statistics (SOS) which has most communication channel information) of the received signals, the unknown input information signals can be recovered successfully.

Various blind adaptive algorithms are discussed throughout this thesis. Simulation results are presented by evaluating the mean square symbol error (MSE) of these techniques to study their performance behavior in blind channel equalization

concept. These algorithms operate blindly in the practical situation, and they can achieve a complete adaptation without the aid of a training sequence, desired response, which is either impractical or very costly. The parameters of equalizer are updated in a recursive way with each single output measurement. Finally, the performance comparisons are realized to show which algorithm is more efficient and robustness to noisy channel model (three classes of channel model are used through thesis's simulation). The aim of this thesis is to improve the performance of a wireless communication channel using various blind adaptive equalization algorithms through computer simulations.

The form and content of this abstract are approved. I recommend its publication.

Approved: Miloje Radenkovic

## **DEDICATION**

*To my dear father,*

*To my affectionate mother,*

*To my dear sister and brothers,*

*To my lovely wife and daughters,*

*who always offer their patience, prayers, support, encouragement and endless love.*

## ACKNOWLEDGMENT

All thanks are offered to Allah who provides me with the help and inspiration to be able to complete this thesis.

I wish to express my sincere thanks and deep gratitude to my supervisor ***Prof. Dr. Miloje Radenkovic*** for his kind advice, helpful, valuable suggestions and continuous encouragement throughout the work for this thesis.

I feel indebted to my family; my gratitude and appreciation are to my father (Qasim) , mother, sister (Zahraa) and my wife (Sarah) who have been a source of motivation and strength during moments of despair and discouragement, and I want to thanks them a lot for offering everything to me to reach this point in my life. Their care and support have been shown in incredible ways recently. I also would like to acknowledge my brothers (Osama and Ahmed) for their encouragement and assistance in order to push my research up to this point.

# TABLE OF CONTENTS

## CHAPTER

I.	INTRODUCTION .....	1
1.1	Introduction and Background Information to Blind Adaptive Equalizer .....	1
1.2	Thesis Overview .....	4
1.3	Mathematical Notations .....	6
II.	MODEL OF COMMUNICATION SYSTEM AND MATHEMATICAL FRAMEWORK .....	10
2.1	Introduction .....	10
2.2	Channel Model .....	12
2.3	Vector Representation .....	16
2.4	Overall System Model with Equalizer .....	18
III.	BLIND ADAPTIVE CHANNEL EQUALIZATION METHODS .....	22
3.1	Adaptive Filter Theory .....	22
3.2	Adaptive Equalization .....	23
3.3	Blind Adaptive Equalization .....	24
3.4	Blind SIMO Channel Equalization Methods Using Second Order Statistics (SOS) .....	24

3.5	Cyclic Statistics .....	25
3.6	Direct Blind MMSE Equalizers .....	27
3.7	Methods for Blind Equalizer Calculation .....	29
3.7.1	Recursive Blind Adaptive Using Recursive Least Square Algorithm (RLS) .....	29
3.7.2	Recursive Blind Adaptive Using Cyclic Least Mean Square Algorithm (cyclic LMS) .....	31
3.7.3	Recursive Blind Adaptive Using Least Mean Square Algorithm (LMS) .....	33
3.7.4	Unbiased Blind Adaptive Using Gradient Projection Technique .....	36
3.7.5	Recursive Blind Adaptive Using Recursive Extended Least Square Algorithm (RELS) .....	38
IV.	PERFORMANCE OF ADAPTIVE BLIND EQUALIZATION ALGORITHMS AND SIMULATIONS .....	45
4.1	Performance Evaluations .....	46
4.1.1	Mean Square Error (MSE) .....	46
4.1.2	Symbols Constellation Plots .....	47
4.2	Simulations .....	48
4.2.1	Experiment 1a .....	48
4.2.2	Experiment 1b .....	52
4.2.3	Experiment 2 .....	55
4.2.4	Experiment 3a .....	57

4.2.5	Experiment 3b .....	58
4.2.6	Experiment 4a .....	62
4.2.7	Experiment 4b .....	64
4.2.8	Experiment 5a .....	66
4.2.9	Experiment 5b .....	68
V.	CONCLUSION .....	<b>72</b>
	REFERENCES .....	<b>74</b>

## LIST OF FIGURES

### FIGURE

2.1	General model of a communication system .....	10
2.2	Basic elements in a digital communication system .....	11
2.3	Fractionally sampled ( $P = 2$ or more) communication system .....	13
2.4	SIMO multichannel model ( $P = 2$ ) .....	15
2.5	Multichannel system models with equalizer $g(n)$ .....	18
3.1	SIMO channel Model (IIR).....	40
3.2	Predictor Based Equalizer .....	40
4.1	Two-ray multipath channel, the magnitude of impulse response $h(n)$ .....	49
4.2	The zeros of $h(n)$ , and the subchannels zeros $h_0(n)$ and $h_1(n)$ .....	50
4.3	Constellation plot of the received sequence for 16 QAM modulation .....	51
4.4	Equalized symbol-eye diagram, using RLS algorithm with the raised-cosine channel .....	51
4.5	Mean-square symbol error of RLS algorithm.....	52

4.6	The magnitude and zeros of impulse response $h(n)$ , second class of channel model .....	53
4.7	Eye diagram of the received signal for 16 QAM modulation .....	54
4.8	Equalizer output symbols, using RLS algorithm with the second class of channel model .....	54
4.9	Mean-square symbol error of RLS algorithm .....	55
4.10	Eye diagram of equalizer output, using cyclic LMS with the raised-cosine channel .....	56
4.11	Mean-square symbol error of cyclic LMS .....	56
4.12	Equalized eye diagram, using LMS algorithm with the raised-cosine channel .....	57
4.13	Mean-square symbol error of LMS algorithm .....	58
4.14	Eye diagram of equalizer output, using LMS algorithm with the second class of channel model .....	59
4.15	Mean-square symbol error of LMS algorithm .....	59
4.16	Mean-square symbol error, Comparison using raised-cosine channel .....	60
4.17	Mean-square symbol error, Comparison using second class of channel model .....	61
4.18	Eye diagram of equalizer output, using LP method with the braised-cosine channel .....	62
4.19	Mean-square symbol error of LP method .....	63

4.20	Eye diagram of equalizer output, using LP algorithm with the second class of channel model .....	64
4.21	Mean-square symbol error of LP algorithm .....	65
4.22	Eye diagram of received signal for 16 QAM modulation .....	67
4.23	Eye diagram of equalizer output, using RELS algorithm with the third class of channel model (IIR) .....	67
4.24	Mean-square symbol error of RELS algorithm .....	68
4.25	Scatter plot of equalized symbols, using RELS algorithm with the presence of modeling error using (IIR) channel .....	69
4.26	Sample mean square error of RELS algorithm .....	70
4.27	Mean-square symbol error, Comparison for those five algorithms with the second class of channel model .....	71

# **CHAPTER I**

## **INTRODUCTION**

### **1.1 Introduction and Background Information to Blind Adaptive Equalizer**

Communication systems have been growing during the past 40 years, and their applications have been used in many electronic products. In these days, radios, televisions, mobiles, and computer terminals with Internet comprise an essential element in our life. They all have ability of providing fast communications from every corner of the globe. We notice that there is an almost unlimited or endless amount of applications relying on the use of communication systems.

Any digital communication system involves transmission of analog signals through channels. These channels are usually dispersive mediums that introduce delay or memory in the received signal, which in turn spreads the symbols over time. This spreading of symbols induces a distortion known as inter-symbol-interference (ISI) [11]. This kind of distortion is undesirable because it makes communication systems less reliable and in order to maintain our systems reliable performance, it must be removed at the receiver by equalization. In many high speed data rates bandlimited digital communication systems, it is shown that ISI appears in all communication channels such as twisted pairs cables, coaxial cables, fiber optics, satellite, microwave and radio channels. This interference between the adjacent symbols corrupts the detection of those symbols since their spreading can corrupt the

time spacing. Increasing ISI causes to increase the error probability at the receiver. Therefore, under strong ISI, a simple memoryless decision device may not be able to recover the original data sequence [7].

ISI needs to be suppressed at the receiver to keep our systems in reliable performance. Equalizers are used as a solution at the receiver to compensate the distortion (ISI) occurring during transmission. Equalizers try to extract the transmitted symbol sequence by countering the effect of ISI. Therefore, they improve the probability of correct symbol detection [16].

One of the earliest channel equalization methods is achieved by sending a training sequence to estimate the linear filtering dispersion characteristics of the nonideal channel (channel identification). Note that the nonideal channel characteristics are usually not known priori, and the training sequence was already known at the receiver. The training sequence is required to be sent periodically since an adaptive channel equalizer relies on it, which occupies much of the bandwidth, resulting lower communication link efficiency. For this reason, a self-recovering approach that does not need a training sequence is invented. Such approach is termed '*blind*'. This idea of self recovering blind equalization was first introduced by Sato in 1975 [7].

In recent few years, many different blind algorithms have been introduced, and it has been growing to the idea of the so-called '*blind problem*' [4], [5], [14], [17] [28] and [29]. In general, blind processing can be defined as a digital processing of

unknown signals that are sent through a linear channel without any knowledge of its characteristics and additive noise. In wireless communications systems, the blind signal processing plays an important role in combating frequency selective fading and inter-symbol interference (ISI) [12]. Blind adaptive equalization methods treat the problem of recovering the transmitted input sequence by using only the received output signal without knowledge of the channel characteristics. Since then, blind channel equalization has obtained great research interest because of the fact that receivers start equalization with no need of transmitter assistance (sending training signals). Consequently, a better channel bandwidth efficiency is obtained.

## 1.2 Thesis Overview

This thesis considers the problem of blind adaptive equalization in communication systems. It starts presenting some introduction to general communication systems and their applications in our daily life. The introduction also explains how the distortion (ISI) is generated and due to its effects on our system's performance, it has to be removed by using equalization. It introduces one of the earliest equalization algorithms (using training sequences) and its drawbacks with respect to valuable performance and throughput, causing to develop the so-called blind equalization techniques. Definition of blind processing and its advantages is also demonstrated in a simple way. Chapter 2 describes the channel model used throughout this thesis. Fractionally sampling scenario is considered in our channel model that is SIMO scheme. It also presents the complete system model (channel with linear equalizer) and their vector forms representation that will be useful for derivations the blind algorithms that are discussed in chapter 3. This chapter ends with discussing the conditions to achieve a perfect equalization.

Chapter 3 begins with the definition of adaptive filter and its applications, including channel equalization. It introduces blind adaptive SIMO channel equalization method (using only second order statistics (SOS) of the received signals to design the equalizer) such as Direct Blind MMSE Equalizers. This chapter also presents the calculation methods for blind equalizer including derivations of Recursive Least Square (RLS), cyclic Least Mean Square (cyclic LMS), Least Mean

Square (LMS), Linear Prediction (using GP technique) and Recursive Extended Least Square (RELS).

Chapter 4 gives simulation results of the equalization techniques to examine their performance behaviors. One of the performance measures is Mean Square Error (MSE) that can be used to compare the equalization algorithms. The channel model classes used through simulations are also described in this chapter. The rest of the chapter is graphs, results, and comparisons between all of these algorithms with respect to their MSE using different classes of channel model. Chapter 5 gives a brief conclusion to the overall concepts included in this thesis.

### 1.3 Mathematical Notations

$w_c(t)$  ..... Continuous-time input information signal

$w(n)$  ..... Input discrete-time sequences

$\hat{w}(n)$  ..... Equalizer output

$\delta(t)$  ..... Dirac delta function

$h_c(t)$  ..... Continuous-time impulse response of composite channel

$h(n)$  ..... Discrete-time equivalent of  $h_c(t)$

$h_0(n), h_1(n)$  ..... Finite-length impulse responses of the two subchannels

$\mathbf{h}$  ..... Vector form of channel impulse response

$\mathbf{h}_0, \mathbf{h}_1$  ..... Vector form of the two subchannels coefficients

$v_c(t)$  ..... Continuous-time additive noise

$v(n)$  ..... Discrete-time equivalent of  $v_c(t)$

$x_c(t)$  ..... Continuous-time channel output

$y_c(t)$  ..... Continuous-time channel output with additive noise

$y(n)$  ..... Received discrete data signal, input to equalizer

$y_0(n), y_1(n)$  ..... Received discrete data signals of the subchannels outputs

$g(n)$ .....	Discrete-time impulse response of linear equalizer
$\mathbf{g}$ .....	Vector form of linear equalizer
$\mathbf{g}_0, \mathbf{g}_1$ .....	Vector forms of the two subequalizers
$T_s$ .....	Pulse duration
$*$ .....	Convolution
$(.)^*$ .....	Complex conjugate
$(.)^T$ .....	Transpose
$(.)^H$ .....	Hermitian or the conjugate transpose
$(.)^\dagger$ .....	Pseudoinverse
$\mathbf{H}^T$ .....	Channel convolution matrix, Sylvester or Block Toeplitz matrix
$C_{2w}(n), C_{2v}(n), C_{2y}(n)$ ..	Correlations of the stationary input, noise, and channel noisy output
$J$ .....	Cost function
$\hat{\nabla} J_0(N)$ .....	The instantaneous approximation to the gradient of the cost function $J_0$
$J(\mathbf{g})$ .....	Prediction error variance
$\ .\ $ .....	Norm or absolute value

$E[.]$ .....	Expected value
$\sigma_w^2$ .....	Input variance
$\sigma_n^2$ .....	The channel noise variance
$\lambda$ .....	Forgetting factor
$\mu, \alpha$ .....	The small step size
$\gamma$ .....	Constraint value
$q^{-1}$ .....	Unit delay operator
$B(q^{-1}), C(q^{-1}), A(q^{-1})$ ..	Polynomials of IIR channels
$F(q^{-1})$ .....	Common factor (minimum phase)
$y(i + 1)$ .....	One step-ahead prediction of $x_1(i + 1)$
$\hat{y}(i + 1)$ .....	A posteriori prediction
$R(q^{-1}), S(q^{-1}), D(q^{-1})$ ..	Polynomials of IIR equalizer
$\hat{\theta}(i)$ .....	An estimate of unknown $\theta_0$
$I$ .....	Identity matrix
$p_0$ .....	An arbitrary finite positive scalar
MSE .....	Mean square error

$\beta$ .....	Roll-off factor
$r_c(t, \beta)$ .....	Raised-cosine channel
$\delta$ .....	A parameter defining the size of the channel modeling error
i.i.d. ....	Independent and identically distributed
FIR, IIR .....	Finite impulse response, Infinite impulse response
SIMO .....	Single input-multiple output
SOS .....	Second order statistics
QAM .....	Quadrature amplitude modulation
LTI .....	Linear time invariant

## CHAPTER II

### MODEL OF COMMUNICATION SYSTEM AND MATHEMATICAL FRAMEWORK

#### 2.1 Introduction

A general and basic model for a communication system is comprised of digital signal that is transmitted by a transmitter through an analog channel to a receiver (see Figure 2.1).



Figure 2.1 General model of a communication system.

Source information may be either a digital or an analog signal. The transmitter is fed from source information, which for the purpose of this thesis we assume is a binary. However, when the information source is an analog signal, transmitter is extended to have a so-called source encoder to convert the analog signal into a sequence of binary digits. This sequence is passed through a channel encoder to introduce a redundancy in the binary information sequence. This redundancy in the binary information is used at the receiver to overcome the effect of noise and interference in the transmission signal through the channel. The binary sequence at the output of the channel encoder is passed to a digital modulator which does the job of mapping the binary information sequence into waveforms to be sent through

communication channels. Figure 2.2 illustrates basic elements in a digital communication system model. The main digital modulation scheme used in the analysis and simulations throughout this thesis is a 16-QAM (quadrature amplitude modulation) since the symbols are usually complex with in-phase and quadrature components. Non ideal analog media such as telephone cables and radio channels typically distort the transmitted signal. During transmission, the essential features of the transmitted signal are corrupted in a random manner.

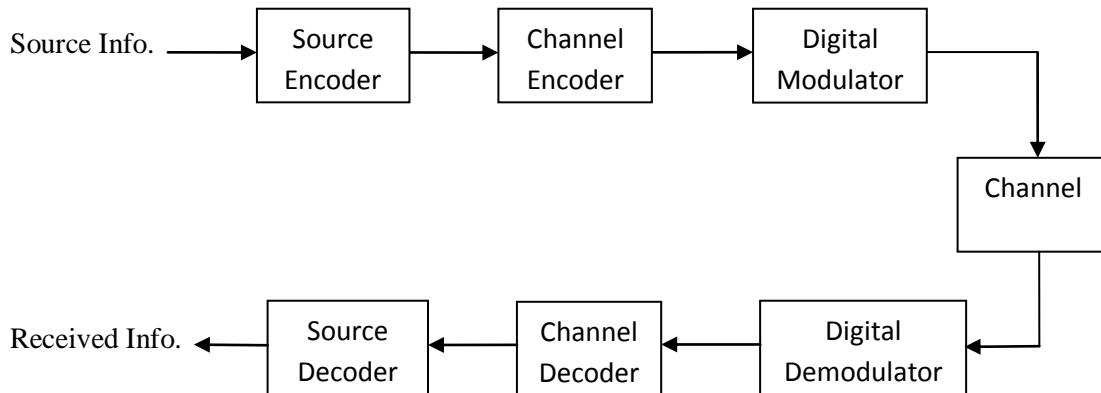


Figure 2.2 Basic elements in a digital communication system.

At the receiver end of a digital communication system, the digital demodulator processes the channel corrupted signal waveform to convert the waveform into a sequence of number that represents the transmitted signal. Then, this sequence is passed through a channel decoder, which attempts to recover the original information sequence. How well the original signal is recovered depends on many

factors such as transmitted signal power, characteristics of the channel, the amount of noise and nature of interference.

QAM 16 and higher is widely used in communication systems, and it combines both phase shift keying (PSK) and amplitude shift keying (ASK) modulations. A simple concept of input-output communication system using M-QAM is that the transmitter generates a sequence of complex-valued random input data  $\{w(l)\}$ , each element of which belongs to a complex alphabet  $A$  (or constellation) of M-QAM symbols. The data sequence  $\{w(l)\}$  is sent through a baseband equivalent unknown complex linear time invariant (LTI) channel whose output  $x(t)$  is observed by the receiver. The function of the receiver is to estimate the original data  $\{w(l)\}$  from the received signal  $x(t)$  [7]. QAM 16 will be used in this thesis because its constellations allow for more bits per symbol and thus more bits per hertz.

## 2.2 Channel Model

In a digital communication system, the transmitter modem takes  $R$  bits of binary data at a time and encodes them into one of  $2^R$  analog symbols for transmission (at the signaling rate) over an analog channel. At the receiver the analog signal is sampled and decoded into the required digital format.

Assume that at the transmitter modem, the  $l^{th}$  set of  $R$  binary digits is mapped into a pulse of duration  $T_s$  seconds and an amplitude  $w(l)$ . Thus the modulator output signal, which is the input to the communication channel, is given as

$$w_c(t) = \sum_l w(l)\delta(t - lT_s). \quad (2.1)$$

where  $w_c(t)$  is the continuous-time information signal,  $\delta(t)$  is a pulse of duration  $T_s$  with an amplitude  $w(l)$ .

The unknown complex-valued LTI communication channel with the impulse response  $h(t)$  composited with the known transmit and receive filters is shown in Figure 2.3. The overall composite channel  $h_c(t)$  is finite impulse response (FIR). Additive noise  $v_c(t)$  that is assumed to be stationary and uncorrelated with the information symbols  $w(n)$  can be included in this model.

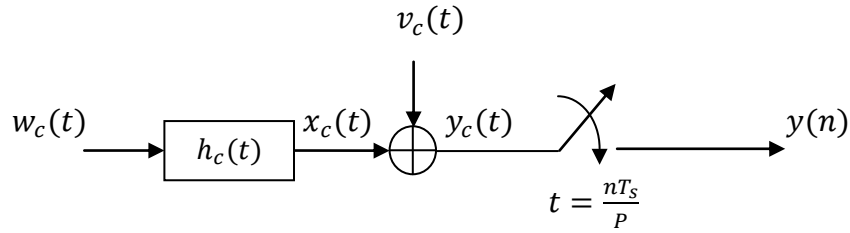


Figure 2.3 Fractionally sampled ( $P = 2$  or more) communication system.

The composite channel (whose impulse response is  $h_c(t)$ ) is non ideal, which means  $h_c(t)$  is nonzero for  $t \neq 0$ . An integer  $P$  in Figure 2.3 denotes the amount of fractionally sampling (oversampling). The channel output can be modeled as the convolution of the input signal and composite channel response. The signal at the sampler is:

$$y_c(t) = (w_c(t) * h_c(t)) + v_c(t),$$

$$y_c(t) = \int_{-\infty}^{\infty} w_c(\tau) h_c(t - \tau) d\tau + v_c(t). \quad (2.2)$$

substituting (2.1) into (2.2), we get

$$y_c(t) = \sum_{l=-\infty}^{\infty} \int_{-\infty}^{\infty} w(l) \delta(\tau - lT_s) h_c(t - \tau) d\tau + v_c(t). \quad (2.3)$$

$$y_c(t) = \sum_l w(l) h_c(t - lT_s) + v_c(t). \quad (2.4)$$

If  $y_c(t)$  is sampled at  $t = nT_s/P$ , the received discrete data signal ( $y(n) \equiv$

$y_c(t)$  for  $t = nT_s/P$ ) is

$$y(n) = \sum_l w(l) h_c\left(nT_s/P - lT_s\right) + v_c(nT_s/P). \quad (2.5)$$

Considering  $w(n)$  and  $y(n)$  are the input and output discrete-time sequences, respectively, it is convenient to rewrite (2.5) as an equivalent discrete-time system

$$\begin{aligned} y(n) &= \sum_{l=-\infty}^{\infty} w(l) h(n - lP) + v(n), \\ &= x(n) + v(n). \end{aligned} \quad (2.6)$$

where  $h(n)$  and  $v(n)$  are the discrete-time equivalents of  $h_c(t)$  and  $v_c(t)$ , respectively,  $x(n)$  is the discrete-time equivalent of the noise free received signal, and index  $n$  can be any integer ( $n = \dots, -3, -2, -1, 0, 1, 2, 3, \dots$ ) [11].

In the single input–multiple output model, an integer  $P > 1$  of measurements are performed for each transmitted symbol, provided the continuous-time observation is oversampled compared with the transmitted symbol rate, leading to create a fractionally spaced scenario. Throughout this thesis, it is assumed that  $P = 2$  to make our model in the oversampling scheme (see Figure 2.4).

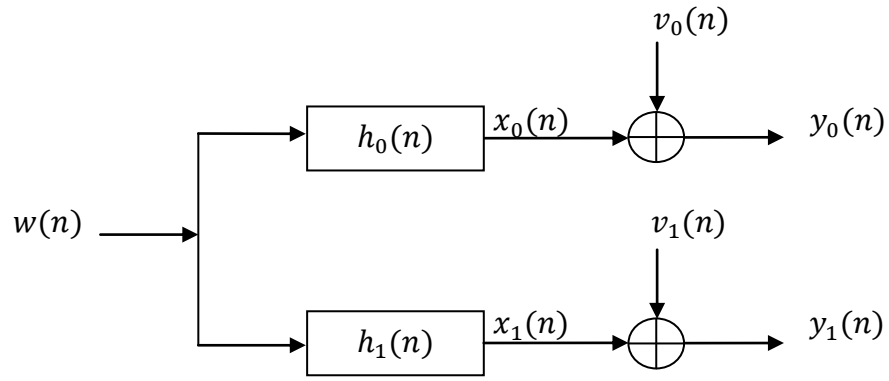


Figure 2.4 SIMO multichannel model ( $P = 2$ ).

now, (2.6) can be rewritten in fractionally spaced system as follows

$$y_i(n) = \sum_{l=-\infty}^{\infty} w(l)h_i(n-l) + v_i(n) \quad \text{for } i = 0, 1 \quad (2.7)$$

with

$$\begin{aligned} y_0(n) &= w(n) * h_0(n) + v_0(n), \\ &= \sum_{l=-\infty}^{\infty} w(l)h_0(n-l) + v_0(n). \end{aligned} \quad (2.8)$$

and

$$\begin{aligned}
y_1(n) &= w(n) * h_1(n) + v_1(n), \\
&= \sum_{l=-\infty}^{\infty} w(l)h_1(n-l) + v_1(n).
\end{aligned} \tag{2.9}$$

Note that  $h_0(n)$  and  $h_1(n)$  are finite-length channel impulse responses of the first and second channels, respectively, at rate  $1/T_s$ .

### 2.3 Vector Representation

A vector representation is very important and useful in our system analysis and equalizer implementation because it makes our finite-length subchannels  $h_0(n)$  and  $h_1(n)$  easy to understand and modify. The input, noise and output such as  $w(n)$ ,  $v(n)$  and  $y(n)$  can be also expressed in vector form. The index  $n$  in these signals is usually infinite length. However, it will be finite-length when it is used as a vector form. Assume that the finite-length channel  $h(n)$  is causal with length  $2L_h$  such that each subchannel has a length  $L_h$ . Considering the following vectors:

$$y(n) = [y_0(n) \ y_1(n)]^T. \tag{2.10}$$

$$v(n) = [v_0(n) \ v_1(n)]^T. \tag{2.11}$$

$$\mathbf{h} = \begin{bmatrix} h_0(0) & h_0(1) & \dots & h_0(L_h - 1) \\ h_1(0) & h_1(1) & \dots & h_1(L_h - 1) \end{bmatrix}. \tag{2.12}$$

with

$$\mathbf{h}_0 = [h_0(0) \ h_0(1) \ \dots \ h_0(L_h - 1)]. \tag{2.13}$$

and

$$\mathbf{h}_1 = [h_1(0) \quad h_1(1) \quad \dots \quad h_1(L_h - 1)]. \quad (2.14)$$

then

$$y(n) = \begin{bmatrix} y_0(n) \\ y_1(n) \end{bmatrix} = \begin{bmatrix} h_0(0) & h_0(1) & \dots & h_0(L_h - 1) \\ h_1(0) & h_1(1) & \dots & h_1(L_h - 1) \end{bmatrix} * \begin{bmatrix} w(n) \\ w(n-1) \\ \vdots \\ w(n - (L_h - 1)) \end{bmatrix} + \begin{bmatrix} v_0(n) \\ v_1(n) \end{bmatrix}. \quad (2.15)$$

or

$$y(n) = \begin{bmatrix} y_0(n) \\ y_1(n) \end{bmatrix} = \begin{bmatrix} \sum_{l=0}^{L_h-1} w(n-l)h_0(l) + v_0(n) \\ \sum_{l=0}^{L_h-1} w(n-l)h_1(l) + v_1(n) \end{bmatrix},$$

$$= \sum_{l=0}^{L_h-1} w(n-l)h(l) + v(n). \quad (2.16)$$

where  $\mathbf{h}$  is a vector form of the two subchannels,  $\mathbf{h}_0$  and  $\mathbf{h}_1$  represent the vector form coefficients of the first and second channels, respectively. The noisy output vector of 1-input/ 2-output causal  $2L_h$  FIR channel filters driven by the input sequence is  $y(n)$ . Note that  $(L_h - 1)$  is the subchannel polynomial order.

## 2.4 Overall System Model with Equalizer

A finite impulse response filter  $g(n)$  as an equalizer with vector parameters  $\mathbf{g}$  is applied to our channel model to make our system into a complete system form (see Figure 2.5). The goal of the equalizer is to remove the distortion caused by channel ISI.

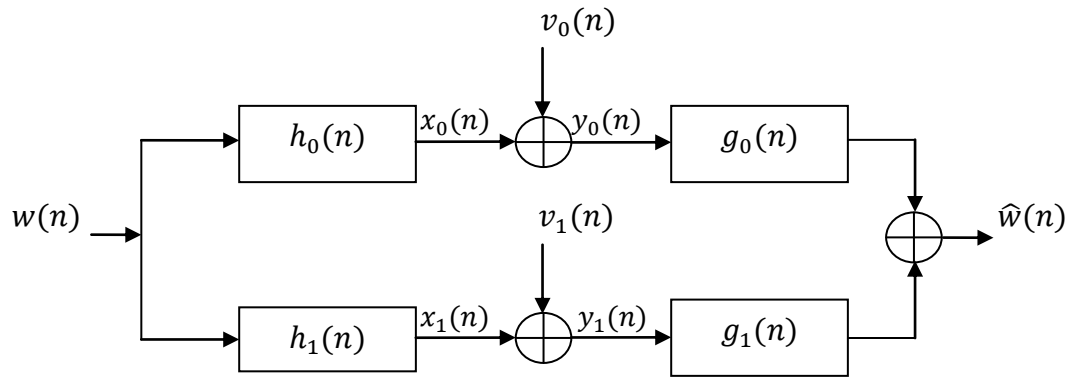


Figure 2.5 Multichannel system models with equalizer  $g(n)$ .

Assume that the finite-length equalizer vector  $\mathbf{g}$  can be defined in a same manner as  $\mathbf{h}$  (as mentioned in previous section) with length  $2L_g$  such that each subequalizer has a length  $L_g$ . The following vectors are defined

$$\mathbf{g} = [g_0(0) \ g_0(1) \ \dots \ g_0(L_g - 1) \ g_1(0) \ g_1(1) \ \dots \ g_1(L_g - 1)]^T. \quad (2.17)$$

with

$$\mathbf{g}_0 = [g_0(0) \ g_0(1) \ \dots \ g_0(L_g - 1)]^T. \quad (2.18)$$

and

$$\mathbf{g}_1 = [g_1(0) \ g_1(1) \ \dots \ g_1(L_g - 1)]^T. \quad (2.19)$$

where  $\mathbf{g}_0$  and  $\mathbf{g}_1$  represent parameter vectors of the first and second equalizers, respectively. Let  $\hat{w}(n)$  be the output signal of equalizer, and then the input-output relationship can be written in the following form

$$\begin{aligned} \hat{w}(n) = & w(n) * [h_0(n) * g_0(n)] + v_0(n) \\ & + w(n) * [h_1(n) * g_1(n)] + v_1(n), \end{aligned} \quad (2.20)$$

$$\begin{aligned} \hat{w}(n) = & w(n) * \left[ \sum_{l=0}^{L_g-1} g_0(l) h_0(n-l) \right] + v_0(n) \\ & + w(n) * \left[ \sum_{l=0}^{L_g-1} g_1(l) h_1(n-l) \right] + v_1(n). \end{aligned} \quad (2.21)$$

To simplify (2.21), let's consider our system in the absence of noise and define  $\mathbf{H}^T$  that is associated with vector  $\mathbf{h}$  to be a channel convolution matrix with the length  $(L_h + L_g - 1) \times PL_g$  as below

$$\mathbf{H}^T = \begin{bmatrix} h_0(0) & 0 & \dots & \dots & 0 \\ h_1(0) & h_0(0) & & & \\ h_0(1) & h_1(0) & h_0(0) & \ddots & 0 \\ \vdots & \vdots & \vdots & \ddots & \vdots \\ h_1(L_h - 1) & h_0(L_h - 1) & \dots & \dots & \vdots \\ \vdots & \vdots & \vdots & \ddots & h_0(L_h - 1) \\ 0 & \dots & \dots & \dots & h_1(L_h - 1) \\ 0 & \dots & \dots & \dots & \dots \end{bmatrix} \quad (2.22)$$

The convolution matrix  $\mathbf{H}^T$  is also called Sylvester or block Toeplitz matrix [15] of the two subchannels, and  $P$  is equivalent to linear filters that the input signal  $w(n)$  passes through ( $P = 2$ ). Alternative representation of (2.22) is found in some books and is written in the following form

$$\mathbf{H}^T = [\mathbf{H}^T_0 : \mathbf{H}^T_1],$$

$$\mathbf{H}^T = \begin{bmatrix} h_0(0) & 0 & \dots & 0 & h_1(0) & 0 & \dots & 0 \\ h_0(1) & h_0(0) & \dots & \vdots & h_1(1) & h_1(0) & \dots & \vdots \\ \vdots & h_0(1) & \ddots & 0 & \vdots & h_1(1) & \ddots & 0 \\ h_0(L_h - 1) & \vdots & \ddots & h_0(0) & \vdots & h_1(L_h - 1) & \ddots & h_1(0) \\ 0 & h_0(L_h - 1) & \vdots & h_0(1) & 0 & h_1(L_h - 1) & \vdots & h_1(1) \\ \vdots & 0 & \ddots & \vdots & \vdots & 0 & \ddots & \vdots \\ 0 & \dots & \dots & h_0(L_h - 1) & 0 & \dots & \dots & h_1(L_h - 1) \end{bmatrix} \quad (2.23)$$

then (2.21) can be written as below

$$\hat{w}(n) = \{\mathbf{H}^T \mathbf{g}\} w(n) = \left\{ [\mathbf{H}^T_0 : \mathbf{H}^T_1] \begin{bmatrix} \mathbf{g}_0 \\ \vdots \\ \mathbf{g}_1 \end{bmatrix} \right\} w(n). \quad (2.24)$$

$$\hat{w}(n) = \left\{ \begin{bmatrix} h_0(0) & 0 & \dots & 0 & h_1(0) & 0 & \dots & 0 \\ h_0(1) & h_0(0) & \dots & \vdots & h_1(1) & h_1(0) & \dots & \vdots \\ \vdots & h_0(1) & \ddots & 0 & \vdots & h_1(1) & \ddots & 0 \\ h_0(L_h - 1) & \vdots & \ddots & h_0(0) & \vdots & h_1(L_h - 1) & \ddots & h_1(0) \\ 0 & h_0(L_h - 1) & \vdots & h_0(1) & 0 & h_1(L_h - 1) & \vdots & h_1(1) \\ \vdots & 0 & \ddots & \vdots & \vdots & 0 & \ddots & \vdots \\ 0 & \dots & \dots & h_0(L_h - 1) & 0 & \dots & \dots & h_1(L_h - 1) \end{bmatrix} \right. \\ \left. \times \begin{bmatrix} g_0(0) \\ g_0(1) \\ \vdots \\ g_0(L_g - 1) \\ \vdots \\ g_1(0) \\ g_1(1) \\ \vdots \\ g_1(L_g - 1) \end{bmatrix} \right\} w(n). \quad (2.25)$$

with

$$w(n) = [w(n) \ w(n-1) \ \dots \ w(n-L_h-L_g+1)]^T. \quad (2.26)$$

where  $\mathbf{H}_0^T$  and  $\mathbf{H}_1^T$  are the convolution matrices of the two subchannels. Note that there is no need to know the channel order  $L_h$  precisely, only the equalizer length  $L_g$  has to be chosen so that the following hypotheses hold in order to have sufficient channel diversity

$H_1)$   $L_h + L_g - 1 < PL_g$  ( $\mathbf{H}^T$  has strictly more columns than rows).

$H_2)$   $\mathbf{H}^T$  has full row rank  $L_h + L_g - 1$  which means the matrix  $\mathbf{H}^T$  is invertible.

The length of equalizer  $L_g$  must be chosen large enough (i.e.  $L_g \geq L_h - 1$ ) in order to have sufficient equations to solve the equalizer. In this case, a perfect equalization can be achieved. It has been shown as in [8], [10], [11], [18], and [24] that the block Toeplitz structure of  $\mathbf{H}^T$  implies that it will be full row rank if and only if there are no common subchannel roots and  $L_g \geq L_h - 1$ . It is also found that there is a unique solution of the equalizer equations if  $L_g = L_h - 1$ .

## **CHAPTER III**

### **BLIND ADAPTIVE CHANNEL EQUALIZATION METHODS**

#### **3.1 Adaptive Filter Theory**

(The beginning of this section is inspired from [13].)

An adaptive filter is defined as a self-designing system that relies for its operation on a recursive algorithm, which makes it possible for the filter to perform satisfactorily in an environment where knowledge of the relevant statistics is not available. Linear and non linear are main groups of adaptive filters. Linear adaptive filters compute an estimate of a desired response by using a linear combination of the available set of observables applied to the input of the filter. Otherwise, the adaptive filter is said to be non linear. In this chapter, adaptive filters theories are described for different kinds of algorithms.

Adaptive filters can be integrated in systems with different functionalities, being predictive deconvolution, system identification, channel equalization, spectral analysis, signal detection, beamforming, interference and noise cancellation examples of such. Also, adaptive filters can adjust to unknown environment, and even track signal or system characteristics varying over time.

### 3.2 Adaptive Equalization

In digital communication systems, one application of adaptive filters is adaptive channel equalization that removes ISI generated from unknown channel. ISI can be compensated or removed from received signals by using many approaches such as optimum receiver which uses maximum likelihood estimation, suboptimum receiver which uses a linear equalizer or a decision-feedback equalizer [20]. The three equalization methods assume impulse response of the channel characteristics or frequency response of the channel characteristics were known a priori to the receiver. However, in most practical digital communication systems that use equalizers the channel characteristics are not known a priori. Therefore, training sequences that provide different realizations of a desired reference signal can be used to estimate the channel and find the necessary equalizer. The reliance of an adaptive channel equalizer on a training sequence requires that the transmitter cooperates by resending the training sequence, lowering the effective data rate of the communication link [7].

In high speed digital communication systems, the transmission of a training sequence is either impractical or very costly in terms of data throughput. Another drawback of using training sequences for channel equalization is that time and bandwidth are consumed for the equalization process, causing most adaptive filters whose desired reference signals are training sequences cannot be used. For these reasons, blind adaptive channel equalization algorithms have been invented and developed, and they have been the best approaches that satisfy our system models.

The purpose of this thesis is applying blind adaptive channel equalization with the variety of algorithms.

### **3.3 Blind Adaptive Equalization**

In some applications, such as multipoint communication networks, the input signal to the channel is unknown to the receiver. Only statistical properties of the input structure that blind equalization based on to recover the unknown input sequence are known. Therefore, it is desirable for the receiver to synchronize the received signal and to adjust the equalizer (self-adaptation) without having a known training sequence available. Equalization techniques based on the initial adjustments of the coefficients without benefit of the training sequence are said to be blind. Now, we can define a blind adaptive filter is an equalizer that uses one of these techniques to perform recursive adjustments of its parameters without the aid of training sequences.

### **3.4 Blind SIMO Channel Equalization Methods Using Second Order Statistics (SOS)**

In the blind methods of equalization, some structure properties of the input signal are used such as whiteness in conjunction with the receiver outputs in order to estimate the equalizer. Also, most commonly used adaptive algorithms for blind channel equalization do not require extra bandwidth for training. Therefore, blind equalizers have gotten great research and practical interest, and many effective algorithms have been proposed for last few years [19] and [23]. In recent papers, ( see for example [3], [18], [26] and [27]), it has been shown that the second order statistics

(SOS) of the channel output  $y(n)$  is sufficient to estimate most communication channels when the received signals are fractionally sampled (oversampling), or multiple antennas are used.

The methods introduced in [9], [10], [11] and [22] have been used SOS of the channel output to directly estimate the equalizer without finding the channel impulse response as a first step. These types of methods are called blind methods. In the following section, the cyclic statistical property of the fractionally sampled observation  $[y(n)]$  is described because some calculation algorithms that will be discussed later in this thesis use this property.

### 3.5 Cyclic Statistics

In this section, we describe the covariance of  $y_N(n)$  which will be useful for finding the equalizers directly from the noise-free channel output. The following vectors are defined to represent  $N$  vector observations of the SIMO fractionally spaced model (see Figure 2.5).

$$y_N(n) = [y_0(n) \ y_0(n-1) \dots y_0(n-N+1) \ y_1(n) \ y_1(n-1) \dots y_1(n-N+1)]^T,$$

$$x_N(n) = [x_0(n) \ x_0(n-1) \dots x_0(n-N+1) \ x_1(n) \ x_1(n-1) \dots x_1(n-N+1)]^T,$$

$$v_N(n) = [v_0(n) \ v_0(n-1) \dots v_0(n-N+1) \ v_1(n) \ v_1(n-1) \dots v_1(n-N+1)]^T. \quad (3.1)$$

The correlation of the scalar output  $y(n)$  in equation (2.6) is defined

$$c_{2y}(n; m) = E\{y(n)y^*(n+m)\}. \quad (3.2)$$

$$c_{2y}(n; m) = \sum_{l_1=-\infty}^{\infty} \sum_{l_2=-\infty}^{\infty} c_{2w}(l_2 - l_1) h(n - 2l_1) h^*(n - 2l_2) + c_{2v}(m). \quad (3.3)$$

where  $m = 0, 1, \dots, L_g - 1$ ,  $c_{2w}(m) \equiv E\{w(n)w^*(n+m)\}$  and  $c_{2v}(v) \equiv E\{v(n)v^*(n+m)\}$  are the correlations of the stationary input and noise, respectively. It can be proven from (3.3) that the correlation is periodically time-varying in  $n$  with period 2, see for proving [25].

$$c_{2y}(n; m) = c_{2y}(n + 2l; m) \ \forall \ l \text{ integer}. \quad (3.4)$$

Due to the periodicity of the correlation matrix, we can use  $y_N(n)$  in similar manner instead of using  $y(n)$  to find the correlation matrix  $C_{2y}^N$  as below

$$C_{2y}^N \equiv E\{y_N(n)y_N(n)^H\}. \quad (3.5)$$

### 3.6 Direct Blind MMSE Equalizers

In this section, we address noise suppression and consider FIR Wiener filters to determine the minimum mean-square sense estimate of equalizer output  $\hat{w}(n)$  using only  $y(n)$ . The objective is to compute the equalizer  $g(n)$  so that the following cost function  $J$  is minimized.

$$J \equiv E\{|\hat{w}(n) - w(n - d)|^2\}. \quad (3.6)$$

where  $d$  is the integer delay between input  $w(n)$  and noise-free channel outputs  $x_i(n)$ ,  $i = 0, 1$ . The output of equalizer  $\hat{w}(n)$  can be written as below

$$\begin{aligned} \hat{w}(n) &= \sum_{l=0}^{L_g-1} g_0(l)y_0(n-l) + \sum_{l=0}^{L_g-1} g_1(l)y_1(n-l), \\ \hat{w}(n) &= \sum_{i=0}^1 \sum_{l=0}^{L_g-1} g_i(l)y_i(n-l). \end{aligned} \quad (3.7)$$

We substitute (3.7) into (3.6) and take the first complex partial derivative with respect to the unknown equalizer coefficients and set it equal zero to minimize  $J$

$$\frac{\partial}{\partial g_k^*(m)} E \left\{ \left| \sum_{i=0}^1 \sum_{l=0}^{L_g-1} g_i(l)y_i(n-l) - w(n-d) \right|^2 \right\} = 0. \quad (3.8)$$

where  $k = 0, 1$  and  $m = 0, 1, \dots, L_g - 1$ . After simplification (see [25]), it yields to orthogonality condition

$$\begin{aligned} \sum_{i=0}^1 \sum_{l=0}^{L_g-1} g_i(l) E\{y_i(n-l)y_k^*(n-m)\} \\ - E\{w(n-d)y_k^*(n-m)\} = 0. \end{aligned} \quad (3.9)$$

Since the input symbols are assumed to be i.i.d., and uncorrelated with the noise, the second term of (3.9) is exist if and only if  $l = n - d$ . Therefore, the second term can be written as follow

$$\begin{aligned}
E\{w(n-d)y_k^*(n-m)\} &= E\left\{w(n-d) \sum_{l=0}^{L_g-1} w^*(l)h_k^*(n-m-l)\right\}, \\
&= E\{w(n-d)w^*(n-d) \\
&\quad \times h_k^*(n-m-(n-d))\}, \\
&= E\{w(n-d)w^*(n-d)\} h_k^*(d-m), \\
&= \sigma_w^2 h_k^*(d-m). \tag{3.10}
\end{aligned}$$

substituting (3.10) into (3.9), yields

$$\begin{aligned}
\sum_{i=0}^1 \sum_{l=0}^{L_g-1} g_i(l)E\{y_i(n-l)y_k^*(n-m)\} - \sigma_w^2 h_k^*(d-m) &= 0, \\
\sum_{i=0}^1 \sum_{l=0}^{L_g-1} g_i(l)E\{y_i(n-l)y_k^*(n-m)\} &= \sigma_w^2 h_k^*(d-m). \tag{3.11}
\end{aligned}$$

the above equation can be written in a vector form as

$$E\left\{y_{L_g}^*(n)y_{L_g}^T(n)\right\}\mathbf{g}_d = \sigma_w^2 \mathbf{H}^*(:, d+1). \tag{3.12}$$

$$C_{2y}^{*N} \mathbf{g}_d = \sigma_w^2 \mathbf{H}^*(:, d+1). \tag{3.13}$$

$$\mathbf{g}_0 = \sigma_w^2 [C_{2y}^{*N}]^\dagger \mathbf{H}^*(:, 1). \tag{3.14}$$

$$\mathbf{g}_d = \sigma_w^2 [\mathbf{C}_{2y}^N]^\dagger \mathbf{C}_{2x,d}^{*N} [\mathbf{C}_{2x}^{*N}]^\dagger \mathbf{H}^*(:, 1). \quad (3.15)$$

The above equations (3.14) and (3.15) give to us the zero-delay MMSE equalizer by substituting  $d = 0$  and the arbitrary nonzero delay ( $d \neq 0$ ) MMSE equalizer.

### 3.7 Methods for Blind Equalizer Calculation

This section introduces and describes five methods for blind equalizer calculation with their derivations. These blind algorithms are procedures for self adjusting the parameters of an adaptive filter to minimize the cost function. We describe the general form of adaptive FIR and IIR filtering concept.

#### 3.7.1 Recursive Blind Adaptive Using Recursive Least Square Algorithm (RLS)

This algorithm addresses the problem of blind adaptive equalization of finite impulse response channels (FIR) with the exploiting the diversity induced by sensors arrays or fractionally sampled. It analyses and solves the case when we have parallel subchannels in the presence or absence of noise. It is shown later that the resulting a priori error converges towards a scalar version of the input symbol sequence and the equalizer parameters are estimated by using Recursive Least Square (RLS) algorithm. This algorithm is very useful for tracking time varying channel. The RLS algorithm uses information from all past input samples (and not only from the current tap-input samples) to estimate the static correlation matrix of the input vector  $\mathbf{C}_{2y}^{*N}$ . To start

driving this algorithm, it is assumed that the additive noise is to be uncorrelated with input samples and a forgetting factor  $\lambda$  ( $0 \leq \lambda \leq 1$ ) is included to reduce the effect of past observations on the statistics correlation matrix estimate  $C_{2y}^{*N}$ .

$$\begin{aligned}\hat{C}_{2y}^*(N) &= E\{y_{L_g}^*(n)y_{L_g}^T(n)\}, \\ &= \sum_{l=0}^N \lambda^{N-l} y_{L_g}^*(l)y_{L_g}^T(l)\end{aligned}$$

At  $l = N$ , the correlation matrix is simplified as

$$\begin{aligned}\hat{C}_{2y}^*(N) &= \sum_{l=0}^{N-1} \lambda^{N-l} y_{L_g}^*(l)y_{L_g}^T(l) + y_{L_g}^*(N)y_{L_g}^T(N) \\ &= \lambda \hat{C}_{2y}^*(N-1) + y_{L_g}^*(N)y_{L_g}^T(N).\end{aligned}\tag{3.16}$$

The result of (3.16) is a recursive form, and it can be applied to (3.14) to find MMSE equalizer  $\mathbf{g}_0$  with zero delay. However, using the matrix inversion lemma [13, p.480], a direct method to find  $\mathbf{g}_0$  is developed without requiring a matrix inverse or pseudoinversion of  $C_{2y}^{*N}$ . This can be done by defining  $P(N) \equiv \left[\hat{C}_{2y}^*(N)\right]^{-1}$  and applying the matrix inversion lemma with (3.16)

$$\begin{aligned}P(N) &= \lambda^{-1}P(N-1) \\ &\quad - \frac{\lambda^{-2}P(N-1)y_{L_g}^*(N-1)y_{L_g}^T(N-1)P(N-1)}{1 + \lambda^{-1}y_{L_g}^T(N-1)P(N-1)y_{L_g}^*(N-1)}.\end{aligned}\tag{3.17}$$

The above equation can be applied to (3.14) to estimate the MMSE zero delay equalizer  $\hat{\mathbf{g}}_0(N)$

$$\hat{\mathbf{g}}_0(N) = P(N) \frac{1-\lambda^{N+1}}{1-\lambda} \sigma_w^2 \mathbf{H}^T(1, :). \quad (3.18)$$

The equalizer estimate form in (3.18) does not require a matrix inverse and, hence, is computationally feasible for adaptive implementation. If  $\lambda = 1$  is chosen, (3.18) provides a method to recursively compute the time invariant equalizer taps, thereby reducing the memory requirements for long data records [11]. It is very important to mention that the convergence of  $\hat{\mathbf{C}}_{2y}(N)$  is affected by the forgetting factor  $\lambda$  and, thereby, it affects the accuracy of the estimator. The forgetting factor  $\lambda$  is usually chosen between [0.98, 1]. The delay MMSE equalizer  $\hat{\mathbf{g}}_a(N)$  can be driven in a similar way using the same above steps in this method.

### **3.7.2 Recursive Blind Adaptive Using Cyclic Least Mean Square Algorithm (cyclic LMS)**

This algorithm also considers the problem of blind adaptive equalization of finite impulse response channels (FIR) with the exploiting the diversity induced by sensors arrays or fractionally sampled. It analyses and solves the case when we have parallel subchannels in the presence or absence of noise. The cyclic LMS algorithm is very popular, and it uses the Stochastic Gradient Descent approach for updating the equalizer coefficients at each symbol. It provides an instantaneous approximation estimate to the gradient vector of the cost function. The goal of the cyclic LMS method is to estimate the equalizer coefficients to achieve the least mean squared

error. It is shown later that the resulting error converges towards a scalar version of the input symbol sequence. The update of the coefficients is performed in the following gradient descent equation

$$\hat{\mathbf{g}}_0(N) = \hat{\mathbf{g}}_0(N-1) - \frac{1}{2}\mu \hat{\nabla} J_0(N). \quad (3.19)$$

where  $\mu$  is the step size parameter which controls the moving distance along the error surface, and  $\hat{\nabla} J_0(N)$  is the instantaneous approximation to the gradient of the cost

function  $J_0 \equiv E\{|\hat{w}(n) - w(n)|^2\}$ .

$$\hat{\nabla} J_0 = \left[ \frac{\partial J_0}{\partial \mathbf{g}_0^*(0)} \quad \frac{\partial J_0}{\partial \mathbf{g}_1^*(0)} \quad \frac{\partial J_0}{\partial \mathbf{g}_0^*(1)} \quad \frac{\partial J_0}{\partial \mathbf{g}_1^*(1)} \quad \dots \quad \frac{\partial J_0}{\partial \mathbf{g}_0^*(L_g-1)} \quad \frac{\partial J_0}{\partial \mathbf{g}_1^*(L_g-1)} \right]^T. \quad (3.20)$$

The equation (3.20) can be simplified in a same manner as in the derivation of the MMSE equalizer (see section 3.6), yields

$$\hat{\nabla} J_0 = E \left\{ \begin{bmatrix} y_{L_g}^* & y_{L_g}^T \end{bmatrix} \mathbf{g}_0 - \sigma_w^2 \mathbf{H}^H(1, :) \right\}. \quad (3.21)$$

as a result, the instantaneous approximation at time  $N$  is obtained by

$$\hat{\nabla} J_0(N) \equiv y_{L_g}^*(N) y_{L_g}^T(N) \hat{\mathbf{g}}_0(N-1) - \sigma_w^2 \mathbf{H}^H(1, :). \quad (3.22)$$

substituting (3.22) into (3.19), yields to the following equation that the equalizer coefficients can be estimated

$$\hat{\mathbf{g}}_0(N) = \hat{\mathbf{g}}_0(N-1) - \frac{1}{2}\mu [y_{L_g}^*(N) y_{L_g}^T(N) \hat{\mathbf{g}}_0(N-1) - \sigma_w^2 \mathbf{H}^H(1, :)] \quad (3.23)$$

The speed of convergence and steady-state performance rely on choosing of the step size  $\mu$ . The convergence analysis issues are not addressed in this thesis, and they have been studied in many papers and books such as [13].

The cyclic LMS algorithm, as we can see through derivation, does not rely on an explicit matrix inverse. Therefore, it is not sensitive to nearly common subchannel roots. In addition, it has extremely low computational complexity, but it has slow convergence [13, pp. 334- 335].

### **3.7.3 Recursive Blind Adaptive Using Least Mean Square Algorithm (LMS)**

The LMS algorithm is widely used in various applications of adaptive filtering due to its computational simplicity. This algorithm is similar to previous section, the step size parameter  $\mu$ , which affects the convergence speed of the LMS, is used to control the moving distance along the error surface. They use information only from the current tap-input symbols. Also, they both depend on the statistics of the input  $w(n)$  and the output  $y(n)$  signals since their updating equations consist of first complex partial derivative to the cost function that has expectation to those two signals. However, this algorithm uses a Steepest-Descent-Based algorithm for updating the equalizer coefficients at each symbol [9].

In section 3.6, the optimal solution for parameters of the adaptive filter is driven. The objective of this optimal (Wiener) solution is to compute the equalizer  $g(n)$  by minimizing the cost function  $J$  relying only on using the observation  $y(n)$ . In

other word, this solution leads to the minimum mean-square error in estimating the reference signal  $w(n)$ . The optimal (Wiener) solution is given by

$$\begin{aligned}\mathbf{g}_0 &= [C_{2y}^{*N}]^\dagger E\{w(n)y^*(n)\}, \\ \mathbf{g}_0 &= \sigma_w^2 [C_{2y}^{*N}]^\dagger \mathbf{H}^*(:,1).\end{aligned}\tag{3.24}$$

where  $C_{2y}^{*N} \equiv E\{y_N^*(n)y_N^T(n)\}$  and let  $p = E\{w(n)y_N^*(n)\}$  which both are unknown. Now, the LMS method updates the equalizer coefficients using a steepest-descent-based algorithm which in turn can be used to search the Wiener solution of equation (3.24) as follows

$$\begin{aligned}\mathbf{g}(n+1) &= \mathbf{g}(n) - \mu \hat{J}(n), \\ \mathbf{g}(n+1) &= \mathbf{g}(n) + 2\mu [\hat{p}(n) - \hat{C}_{2y}^{*N}(n)\mathbf{g}(n)].\end{aligned}\tag{3.25}$$

where  $\hat{J}(n)$  is an instantaneous estimate to the gradient vector of the cost function with respect to the filter coefficients. Employing instantaneous approximation estimates  $\hat{C}_{2y}^{*N}(n)$  and  $\hat{p}(n)$  for  $C_{2y}^{*N}$  and  $p$  is one possible solution to estimate the gradient vector as follow

$$\hat{C}_{2y}^{*N}(n) = y_N^*(n)y_N^T(n).\tag{3.26}$$

$$\hat{p}(n) = w(n)y_N^*(n).\tag{3.27}$$

The gradient estimate is given by

$$\begin{aligned}
\hat{J}(n) &= -2[\hat{p}(n) - \hat{C}_{2y}^{*N}(n)\mathbf{g}(n)] \\
&= -2w(n)y_N^*(n) + 2y_N^*(n)y_N^T(n)\mathbf{g}(n) \\
&= -2y_N^*(n)[w(n) - y_N^T(n)\mathbf{g}(n)] \\
&= -2y_N^*(n)err(n).
\end{aligned} \tag{3.28}$$

This can be applied back to (3.25), the resulting is the updating equalizer parameters estimate of the least mean square LMS algorithm. In summary, the updating equations for the LMS algorithm are described by

$$err(n) = w(n) - y_N^T(n)\mathbf{g}(n). \tag{3.29}$$

$$\mathbf{g}(n+1) = \mathbf{g}(n) + 2\mu y_N^*(n)err(n). \tag{3.30}$$

The LMS coefficients update which is illustrated in the equation (3.30) is a form of time-averaging that smooth the errors in the instantaneous gradient calculation to obtain a more reasonable estimate of the true gradient [9].

### 3.7.4 Unbiased Blind Adaptive Using Gradient Projection Technique

This algorithm considers the problem of blind adaptive equalization of finite impulse response channels (FIR) with the exploiting the diversity induced by sensors arrays or fractionally sampled. It analyses and solves the case when we have parallel subchannels in a noisy environment. An adaptive equalizer is developed depending on the FIR quadratically constrained filter which uses the Gradient Projection (GP) technique as a solution for its implementation at the receiver. It has been shown that the (GP) technique as described for example in the work by [6] is the most direct solution to the adaptive implementation of quadratically constrained filters. Also, the Gradient Projection algorithm can be used in adaptive beamforming problems at low cost sense [10]. It is shown later that the resulting prediction error converges towards a scalar version of the input symbol sequence and the adaptive filter parameters are estimated by using (GP) algorithm. In addition, the additive noise is assumed to be uncorrelated with input samples.

In order to start driving this method, recall from chapter two that there is no need to know the channel order  $L_h$  precisely, only the equalizer length  $L_g$  has to be chosen such that the following hypotheses hold in order to have sufficient channel diversity

$H_1)$   $L_h + L_g - 1 < PL_g$  ( $\mathbf{H}^T$  has strictly more columns than rows).

$H_2)$   $\mathbf{H}^T$  has full row rank  $L_h + L_g - 1$  which means the matrix  $\mathbf{H}^T$  is invertible.

The notion of linear prediction method (LP) is whitening the observation to find a channel inverse filter, using the following a priori constraint:

$H_3$ ) The input sequence  $w(n)$  is white,  $E\{w(n)w^*(n-k)\} = \delta_k$ .

It is a good point to mention that there is limitation in the SISO case because the whiteness constraint is too weak to allow phase and amplitude equalization of a mixed-phase channel. However, in the SIMO model, this limitation vanishes due to hypotheses  $H_1$  and  $H_2$ , so the exact FIR inverse of the nonideal channel exists. It has been shown in [10] and [24] that the resulting noise-free prediction error signal related to the input symbol sequence  $w(n)$ .

Assume that the finite-length equalizer vector  $\mathbf{g}$  be a  $2L_g \times 1$  complex-valued vector of prediction coefficients, and  $err_k(n)$  be the prediction error defined for  $k = 0, 1$ . The prediction error achieves its optimality in the noise free case if and only if  $err_k(n) = h_k(0)w(n)$ , and thus the prediction error variance  $J(\mathbf{g}) = E|err_k(n)|^2$  is minimized. The performance versus SNR of this theoretical equalization method would critically depend on the realization of the particular coefficient  $h_k(0)$ , so it is more appropriate to exploit the predictor as a tool to identify the channel [10]. A major drawback of the prediction error filtering is sensitivity to channel additive noise. For this reason, a modified prediction scheme will be introduced to allow the adaptive computation of an unbiased predictor in a noisy environment. Adaptive filter parameters are estimated by using the Gradient Projection technique. The algorithm which is first introduced by [10] goes as follows:

$$err_k(n) = y_k(n) - \mathbf{g}(n-1)^H y_N(n-1). \quad (3.31)$$

$$u_k(n) = y_N(n-1)err_k(n)^*. \quad (3.32)$$

$$\tilde{\mathbf{g}}(n) = \mathbf{g}(n-1) + \alpha u_k(n). \quad (3.33)$$

$$\mathbf{g}(n) = \tilde{\mathbf{g}}(n)\gamma / \|\tilde{\mathbf{g}}(n)\|. \quad (3.34)$$

where  $\alpha$  is a small step size and  $\gamma$  is a constraint value. The performance behavior of the mean square error is influenced by the choice of  $\gamma$  in this particular algorithm. It is not difficult to see that (3.33) is a standard LMS update of equalizer parameters. This algorithm has a very low computational cost, and it shows desirable robustness properties [10].

### 3.7.5 Recursive Blind Adaptive Using Recursive Extended Least Square Algorithm (RELS)

This algorithm considers the problem of blind adaptive equalization of *infinite impulse response (IIR) channels* without requiring the channel diversity condition, and it analyses and solves the case when we have parallel subchannels having common zeros. This common factor is assumed as a minimum phase filter, while overall subchannels can be a non minimum phase systems. An equalizer is developed based on the optimal IIR filter as a predictor of the received signal. The main criterion of this method is a one-step ahead prediction of one of the subchannel outputs [1], [2], [10] and [22]. It is shown that the resulting prediction error converges towards a scalar version of the input symbol sequence and the adaptive predictor parameters are

estimated by using Recursive Extended Least Squares (RELS) Algorithm. In addition, it is assumed that the input samples are mutually uncorrelated, and the parameter estimates are updated when each single signal is received [22].

### **Prediction -Based Equalizer**

Consider the case of single-input two-output system model which means the receiver performs two measurements for each transmitted symbol. An equivalent representation to our channel model is shown in Figure 3.1.

$$\begin{aligned} x_1(i) &= \frac{B(q^{-1})F(q^{-1})}{A(q^{-1})} w(i), \\ x_2(i) &= \frac{C(q^{-1})F(q^{-1})}{A(q^{-1})} w(i). \end{aligned} \quad (3.35)$$

where  $q^{-1}$  is a unit delay operator,  $w(i)$  is the transmitted symbol and

$$\begin{aligned} A(q^{-1}) &= 1 + a_1 q^{-1} + \dots + a_L q^{-L}, \\ B(q^{-1}) &= b_0 + b_1 q^{-1} + \dots + b_L q^{-L}, \\ C(q^{-1}) &= c_0 + c_1 q^{-1} + \dots + c_L q^{-L}, \\ F(q^{-1}) &= 1 + f_1 q^{-1} + \dots + f_{n_F} q^{-n_F}. \end{aligned} \quad (3.36)$$

where  $L$  is the polynomial channel order. Assuming that polynomials  $A(q^{-1})$ ,  $B(q^{-1})$ , and  $C(q^{-1})$  are of the same order, and assuming that  $1/A(q^{-1})$  is a stable operator. Also,  $B(q^{-1})$  and  $C(q^{-1})$  are coprime polynomials as well as  $F(q^{-1})$  is a

minimum phase polynomial. In general, all quantities in (3.35) and (3.36) can be complex numbers.

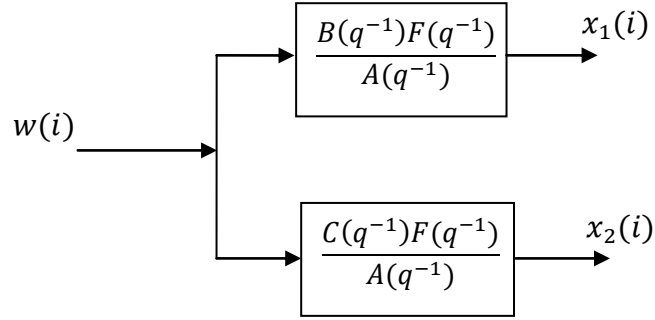


Figure 3.1 SIMO channel model (IIR).

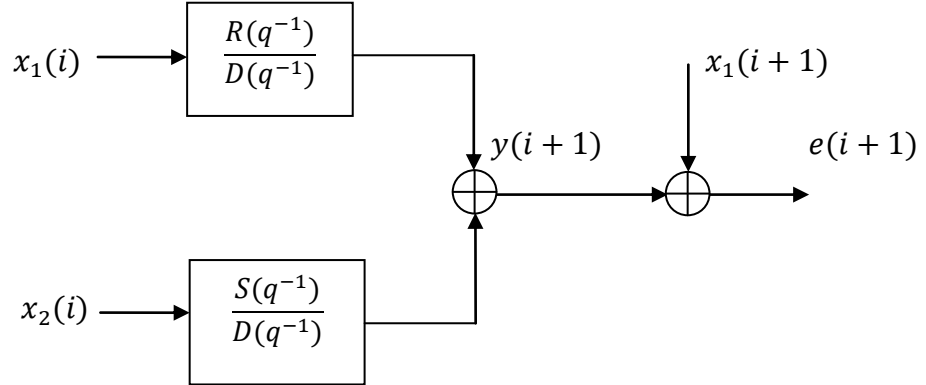


Figure 3.2 Predictor based equalizer.

The prediction-based equalizer is shown in Figure 3.2, where  $y(i + 1)$  is one step-ahead prediction of  $x_1(i + 1)$ . Let  $R(q^{-1})$ ,  $S(q^{-1})$  and  $D(q^{-1})$  be the filter operators and the polynomials in  $q^{-1}$ , so  $y(i + 1)$  is

$$y(i + 1) = \frac{R(q^{-1})}{D(q^{-1})}x_1(i) + \frac{S(q^{-1})}{D(q^{-1})}x_2(i). \quad (3.37)$$

which is optimal in the mean-square sense. The polynomials  $R(q^{-1})$ ,  $S(q^{-1})$  and  $D(q^{-1})$  are computed by minimizing the following cost function  $J$  :

$$J = E(|x_1(i + 1) - y(i + 1)|^2). \quad (3.38)$$

Note that we can use  $x_2(i)$  instead of  $x_1(i)$  as a reference signal and find the predictor by minimizing  $E(|x_2(i + 1) - y(i + 1)|^2)$ . From (3.35) and (3.37),  $x_1(i + 1)$  can be written in the following form

$$x_1(i + 1) - y(i + 1) = -x(i) + b_0w(i + 1). \quad (3.39)$$

where

$$x(i) = H(q^{-1})w(i). \quad (3.40)$$

and

$$H(q^{-1}) = \frac{[B(q^{-1})R(q^{-1}) + C(q^{-1})S(q^{-1})]F(q^{-1})}{A(q^{-1})D(q^{-1})} - \frac{q[B(q^{-1})F(q^{-1}) - A(q^{-1})b_0]}{A(q^{-1})}. \quad (3.41)$$

since  $F(q^{-1})$  is not a factor of  $A(q^{-1})$ , from (3.41) it follows that  $H(q^{-1})=0$  if and only if  $D(q^{-1}) = F(q^{-1})$  whereas  $R(q^{-1})$  and  $S(q^{-1})$  are solutions of the following polynomial equation:

$$\begin{aligned} [B(q^{-1})R(q^{-1}) + C(q^{-1})S(q^{-1})] \\ = q[B(q^{-1})F(q^{-1}) - A(q^{-1})b_0] \end{aligned} \quad (3.42)$$

notice also that  $H(q^{-1}) = 0$  gives  $x(i) = 0$  and from (3.39), we get the prediction error

$$x_1(i+1) - y(i+1) = b_0 w(i+1). \quad (3.43)$$

Let the predictor operators  $R(q^{-1})$  and  $S(q^{-1})$  are defined as

$$\begin{aligned} R(q^{-1}) &= r_0 + r_1 q^{-1} + \dots + r_{N_1} q^{-N_1}, \\ S(q^{-1}) &= s_0 + s_1 q^{-1} + \dots + s_{N_2} q^{-N_2}. \end{aligned} \quad (3.44)$$

Then (3.42) has a solution with respect to  $R(q^{-1})$  and  $S(q^{-1})$  if  $N_1 \geq N_0$ ,  $N_2 \geq N_0$ , where  $N_0 = \max(L-1, nF-1)$ . A unique solution exists if  $B(q^{-1})$  and  $C(q^{-1})$  are coprime,  $L \geq nF$  and at least one of the following holds:  $N_1 = N_0$  or  $N_2 = N_0$ .

In practice, we cannot use (3.42) to calculate  $R(q^{-1})$ ,  $S(q^{-1})$  and  $D(q^{-1})$  since polynomials  $B(q^{-1})$ ,  $C(q^{-1})$  and  $F(q^{-1})$  are unknown. Therefore, we cannot use a nonadaptive predictor (3.37) to calculate prediction error (3.43). A recursive algorithm is proposed for directly estimating the unknown parameters in (3.37).

Taking advantage to our assumption that  $D(q^{-1}) = F(q^{-1})$ , the nonadaptive predictor (3.37) can be written in the form

$$F(q^{-1})y(i+1) = R(q^{-1})x_1(i) + S(q^{-1})x_2(i). \quad (3.45)$$

Let

$$\begin{aligned} \phi_0(i)^T = [x_1(i), \dots, x_1(i - N_1), x_2(i), \\ \dots, x_2(i - N_2), -y(i), \dots, -y(i - N_3)], \quad N_3 \geq nF - 1, \end{aligned} \quad (3.46)$$

and

$$\theta_0^H = [r_0, \dots, r_{N_1}, s_0, \dots, s_{N_2}, f_1, \dots, f_{nF}, 0, \dots, 0]. \quad (3.47)$$

Then (3.45) becomes

$$y(i+1) = \theta_0^H \phi_0(i). \quad (3.48)$$

The number of inserted zeros in (3.47) relies on the value of  $N_3$  and the unknown degree  $nF$ . Equation (3.48) is called the optimal nonadaptive prediction because  $\theta_0$  is unknown. Therefore, the following adaptive predictor can be used

$$\hat{y}(i+1) = \hat{\theta}(i+1)^H \phi(i). \quad (3.49)$$

where  $\hat{\theta}(i)$  is an estimate of unknown  $\theta_0$ , and

$$\begin{aligned} \phi(i)^T = [x_1(i), \dots, x_1(i - N_1), x_2(i), \\ \dots, x_2(i - N_2), -\hat{y}(i), \dots, -\hat{y}(i - N_3)]. \end{aligned} \quad (3.50)$$

Equation (3.49) is called a posteriori prediction, whereas  $\check{y}(i+1) = \hat{\theta}(i)^H \phi(i)$  represents a priori prediction. A priori prediction error  $x_1(i+1) - \check{y}(i+1)$  is used to run the following extended least squares algorithm (first presented by [22]):

$$\hat{\theta}(i+1) = \hat{\theta}(i) + p(i)\phi(i)e(i+1)^*, \quad (3.51)$$

$$e(i+1) = x_1(i+1) - \hat{\theta}(i)^H \phi(i), \quad (3.52)$$

$$p(i) = p(i-1) - \frac{p(i-1)\phi(i)\phi(i)^H p(i-1)}{1 + \phi(i)^H p(i-1)\phi(i)}. \quad (3.53)$$

$$p(0) = p_0 \mathbf{I}, \quad p_0 > 0,$$

where  $\mathbf{I}$  is the identity matrix, and  $p_0$  is an arbitrary finite positive scalar. Initial values of  $\hat{\theta}(0)$  in (3.51) and  $\hat{y}(k)$ ,  $k \leq 0$  in (3.50) are chosen arbitrary. Predictor coefficients are directly computed using the RELS algorithm (3.49)-(3.53). There is no need to know the channel order  $L$  and  $nF$  precisely, as long as one overfit, i.e., in (3.50),  $N_1 \geq N_0$ ,  $N_2 \geq N_0$ ,  $N_0 = \max(L-1, nF-1)$ , and  $N_3 \geq nF$  [22].

## CHAPTER IV

### PERFORMANCE OF ADAPTIVE BLIND EQUALIZATION ALGORITHMS AND SIMULATIONS

This section presents the results of simulations using MATLAB to examine the performance behaviors of various adaptive /recursive algorithms described in chapter 3. The performance of adaptive blind algorithms is assessed through this thesis by calculating the mean-square-error (MSE), and showing constellation plots of each single method. The major mean of comparison is the error cancellation capability using algorithms that rely on the parameters such as step size  $\mu$ , forgetting factor  $\lambda$ , number of iterations and their MSE performance. The principle advantage of these algorithms is to remove ISI, which is generated during transmission, by equalizing the transmission channels, or we can say in a more fashionable way it is to reduce the error probability in the decision at the receiver. The calculation methods that will be simulated in this chapter are cyclic LMS, LMS, RLS, Linear Prediction (using GP technique) and RELS. Before the simulation results are presented, it is useful to look at the brief explanation to the MSE and symbol constellations as performance measures in the following section.

## 4.1 Performance Evaluations

### 4.1.1 Mean Square Error (MSE)

In general, the minimum mean square error (MSE) is a metric indicating how well a system can adapt to a given solution. A small minimum MSE is an indication that the adaptive system has accurately modeled, predicted, adapted, and/or converged to a solution for the system. In other words, the algorithms will achieve better performance. A very large MSE usually indicates that the adaptive filter cannot accurately model the given system, or the initial state of the adaptive filter is an inadequate starting point to cause the adaptive filter to converge. The ideal MSE is when it reaches zero. However, most real systems cannot achieve the ideality. The MSE is defined in a similar form as a cost function in (3.6)

$$MSE \equiv E\{|\hat{w}(n-d) - w(n)|^2\}. \quad (4.1)$$

This equation can be simplified and used in practice by a consistent sample estimate based on  $N$  observations

$$MSE(N) = \frac{1}{N} \sum_{n=0}^{N-1} |\hat{w}(n-d) - w(n)|^2. \quad (4.2)$$

where  $d$  is the desired delay. Most of the time, the graphs illustrate the MSE versus time index samples. The MSE achieves its asymptotic steady state level after a sufficient number of symbols.

#### **4.1.2 Symbols Constellation Plots**

It is also called scatter or eye diagram. This type of performance measures is usually useful to see if the algorithm used is working or not. It is a constellation diagram of the observed signals and equalizers outputs.

## 4.2 Simulations

In this section, the simulation results are presented for all adaptive /recursive methods that were discussed in the previous chapter. The calculation methods that include cyclic LMS, LMS, RLS, LP and RELS are simulated using MATLAB. Some experiments assumed that the input signal is independent and identically distributed (i.i.d.) sequence with the zero mean and unit variance; however, other experiments do not exploit this identity. Nine experiments will be performed in the following nine sections such that each section includes graphs and results related to each single calculation method.

### 4.2.1 Experiment 1a

In this experiment, an i.i.d. symbol sequence that is generated from a 16 QAM constellation is used. The symbol levels along both axes are -1.5, -0.5, 0.5 and 1.5. The continuous time channel that will be the first class of channel model used in the simulation of this thesis spans four symbols and describes for  $t \in [0, 4T_s)$

$$h_c(t) = e^{-j2\pi(0.15)}r_c(t - 0.25T_s, \beta) + 0.8e^{-j2\pi(0.6)}r_c(t - T_s, \beta). \quad (4.3)$$

where  $r_c(t, \beta)$  is the raised cosine given in [20, pp.546] as

$$r_c(t, \beta) = \text{sinc}\left(\frac{\pi t}{T_s}\right) \frac{\cos\left(\frac{\pi \beta t}{T_s}\right)}{1 - 4\beta^2 t^2 / T_s^2}. \quad (4.4)$$

with roll-off factor  $\beta$ , while  $T_s$  is the symbol duration. As in [11],  $\beta = 0.35$  is chosen.

The above  $h_c(t)$  represents the composite causal approximation of a two-ray multipath mobile radio environment. This channel is reported by [1] and [21]. The discrete-time equivalent channel  $h(n)$  is obtained by oversampling ( $P = 2$ )  $h_c(t)$  at a rate of  $T_s/2$  (fractionally sampled) or  $h(n) \equiv h_c(nT_s/2)$  for  $n = 0, 1, \dots, 7$ . Figure 4.1 shows the magnitude of the impulse response  $h(n)$  while Figure 4.2 shows the zeros of  $h(n)$ , and the zeros of the subchannels  $h_0(n)$  and  $h_1(n)$ . The subchannels parameters are

$$\mathbf{h}_0 = [0.52 - j0.72 \quad -0.48 + j0.24 \quad -0.05 + j0.07 \quad 0.01 - j0.02]^T. \quad (4.5)$$

$$\mathbf{h}_1 = [0.12 - j0.43 \quad -0.48 + j0.41 \quad 0.13 - j0.11 \quad -0.04 + j0.03]^T. \quad (4.6)$$

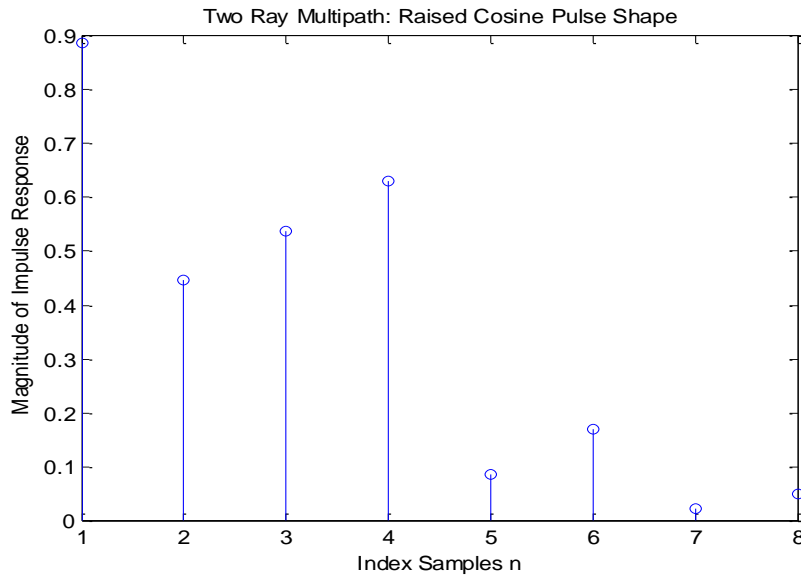


Figure 4.1 Two-ray multipath channel, the magnitude of impulse response  $h(n)$ .

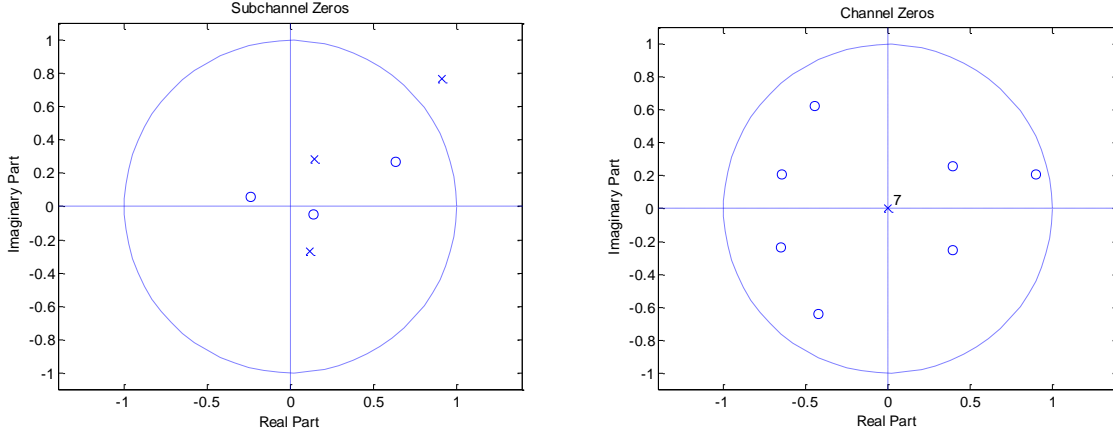


Figure 4.2 The zeros of  $h(n)$ , and the subchannels zeros  $h_0(n)$  and  $h_1(n)$ .

Both Figures 4.1 and 4.2 are first presented in [11]. Using this type of channel to implement the first equalizer calculation method that is Recursive Least Square (RLS) with zero delay ( $d = 0$ ). It is assumed that the subchannel length  $L_h = 4$ , and subequalizer length  $L_g = 4$ . The received constellation is presented in Figure 4.3, while Figure 4.4 shows the equalized eye diagram. Also, Figure 4.5 depicts the mean-square symbol error for RLS algorithm across 3000 symbols. All of these figures in the presence of the receiver noise  $v(n)$  that is assumed to be white with zero mean and 0.14 variance. The performance of RLS algorithm depends on the forgetting factor  $\lambda$  which in this experiment is chosen to be 0.99. For simulation, use equations (3.17) and (3.18).

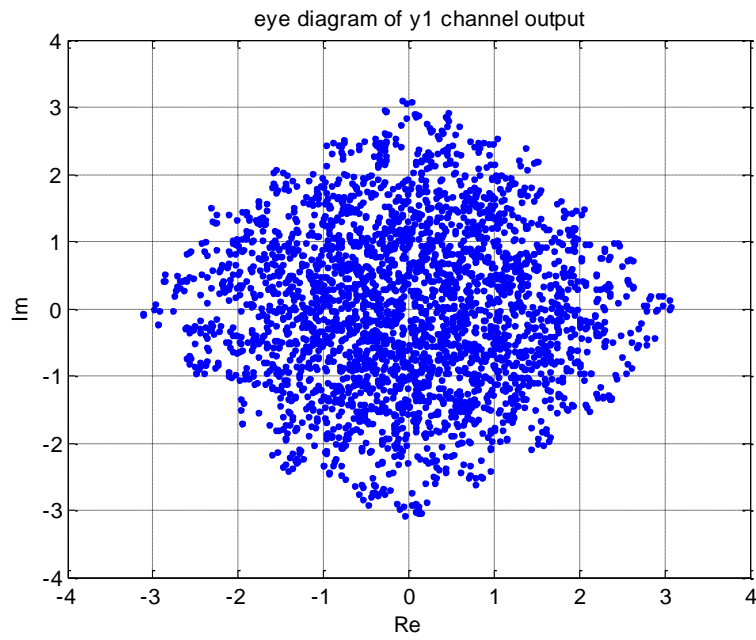


Figure 4.3 Constellation plot of the received sequence for 16 QAM modulation.

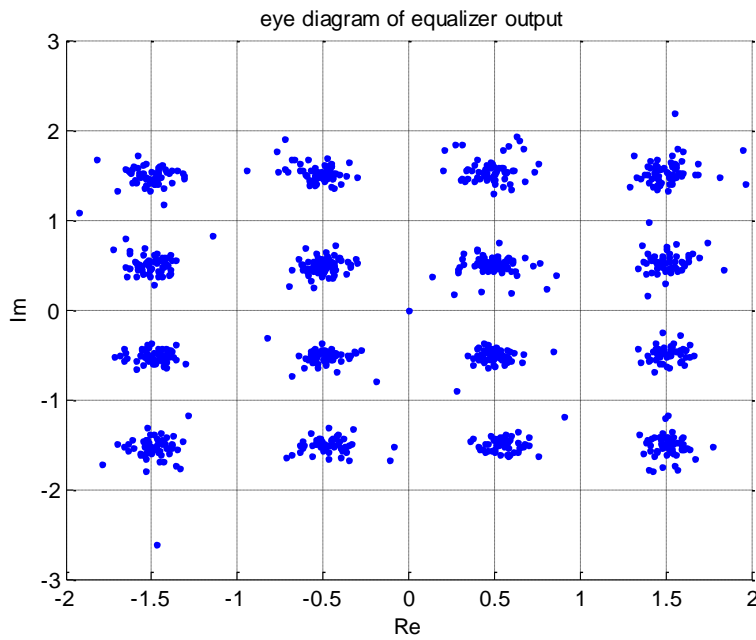


Figure 4.4 Equalized symbol-eye diagram, using RLS algorithm with the raised-cosine channel.

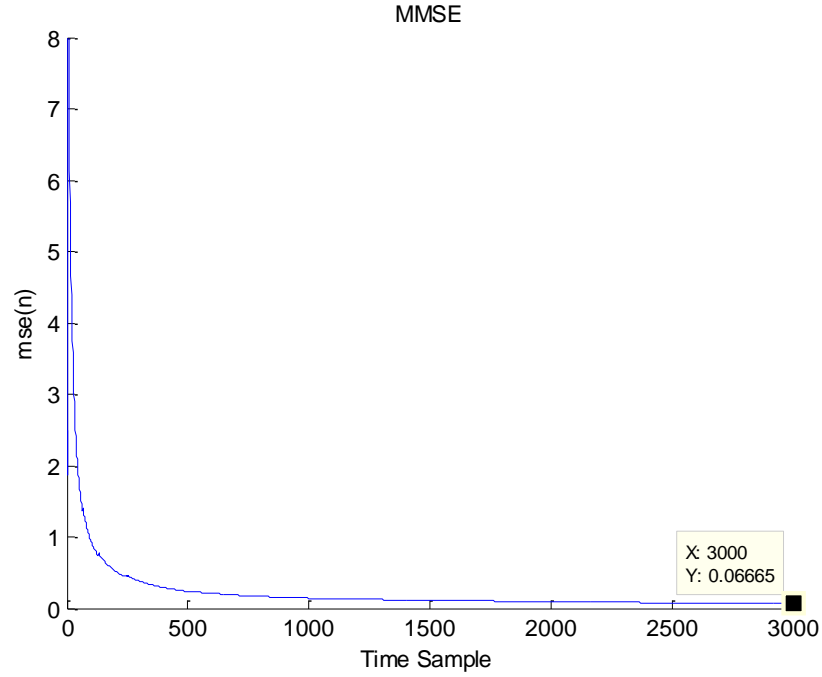


Figure 4.5 Mean-square symbol error of RLS algorithm.

We can see from Figure 4.5 that this algorithm does a very good job of equalization after as few as 1000 symbols. The MSE converges to 0.06665 at index sample  $n = 3000$ .

#### 4.2.2 Experiment 1b

In this section, an uncorrelated symbol sequence generated from a 16- QAM constellation is used. The channel model (second class), which is used in this experiment, is reported by [22], and it has different coefficients than the previous experiment. Figure 4.6 shows the magnitude and zeros of the impulse response  $h(n)$ . The subchannels parameters are described as follow:

$$\mathbf{h}_0 = [0.5498 - j0.3174 \quad 0.4342 - j0.4596 \quad 0.0131 - j0.0919 \\ -0.0275 + j0.1592]^T. \quad (4.7)$$

$$\mathbf{h}_1 = [0.0414 - j0.0717 \quad 0.7168 - j0.3407 \quad 0.0745 - j0.3636 \\ 0.0685 - j0.1861]^T. \quad (4.8)$$

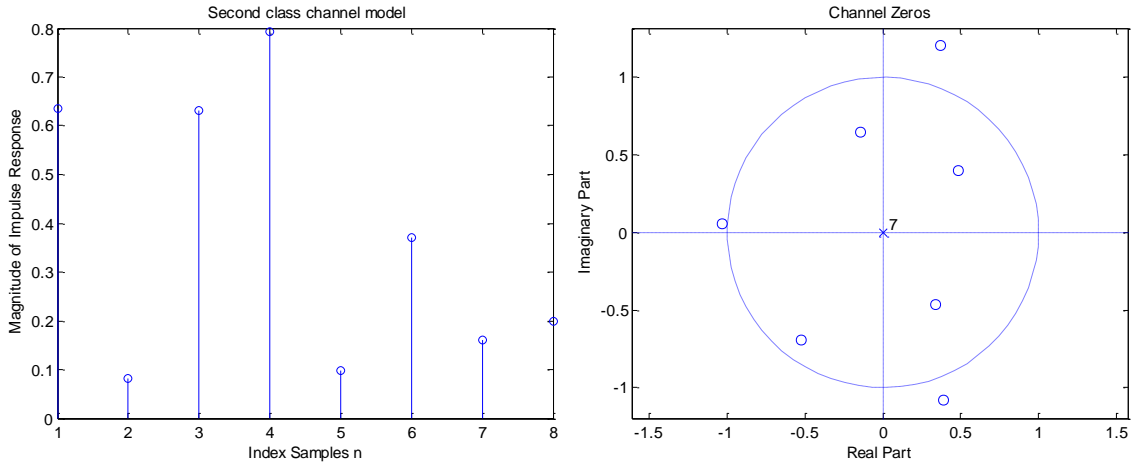


Figure 4.6 The magnitude and zeros of impulse response  $h(n)$ , second class of channel model.

The RLS algorithm is implemented again using the second class of channel model with zero delay ( $d = 0$ ). It is assumed that the subchannel length  $L_h = 4$ , and subequalizer length  $L_g = 4$ . The received symbols are presented in Figure 4.7, while Figure 4.8 shows the equalized constellation. Also, the mean-square symbol error is estimated for this algorithm across 3000 symbols as shown in Figure 4.9. All of these figures in the presence of the additive noise  $v(n)$  that is assumed to be white with zero mean and 0.14 variance. The forgetting factor  $\lambda$  is also 0.99.

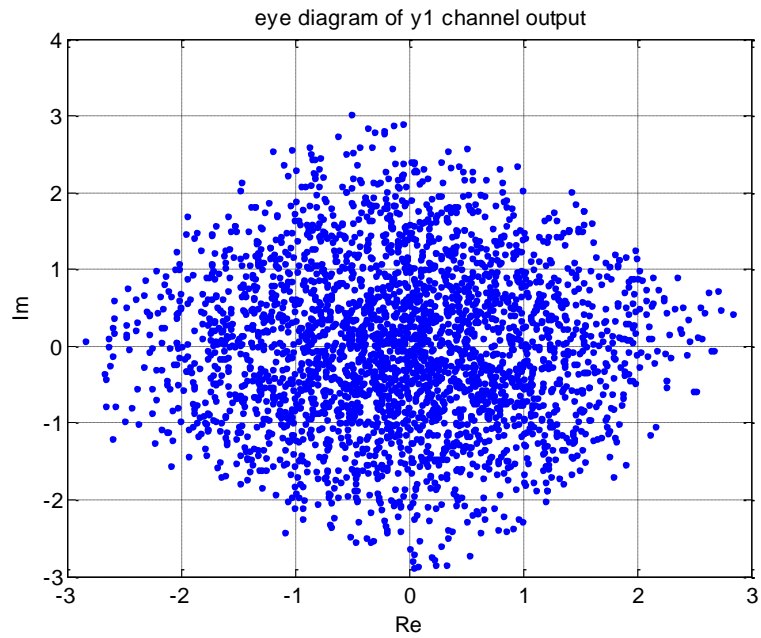


Figure 4.7 Eye diagram of the received signal for 16 QAM modulation.

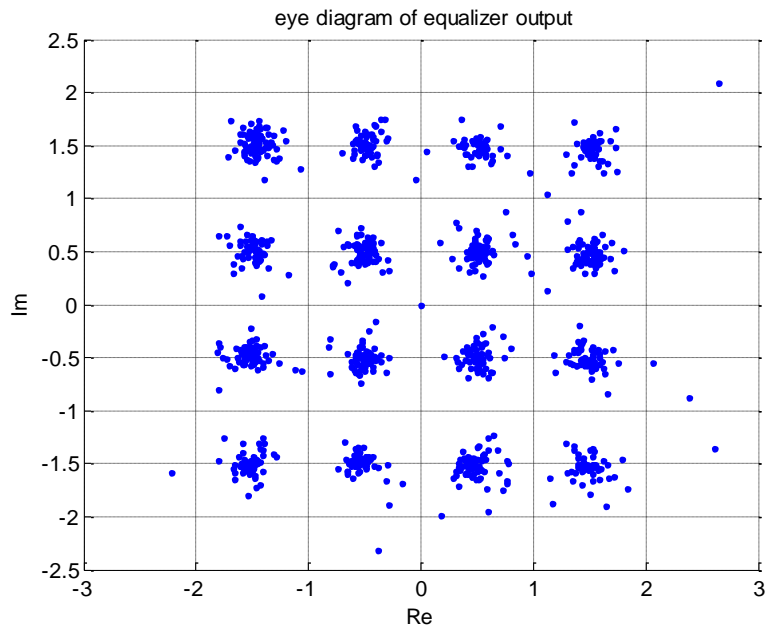


Figure 4.8 Equalizer output symbols, using RLS algorithm with the second class of channel model.

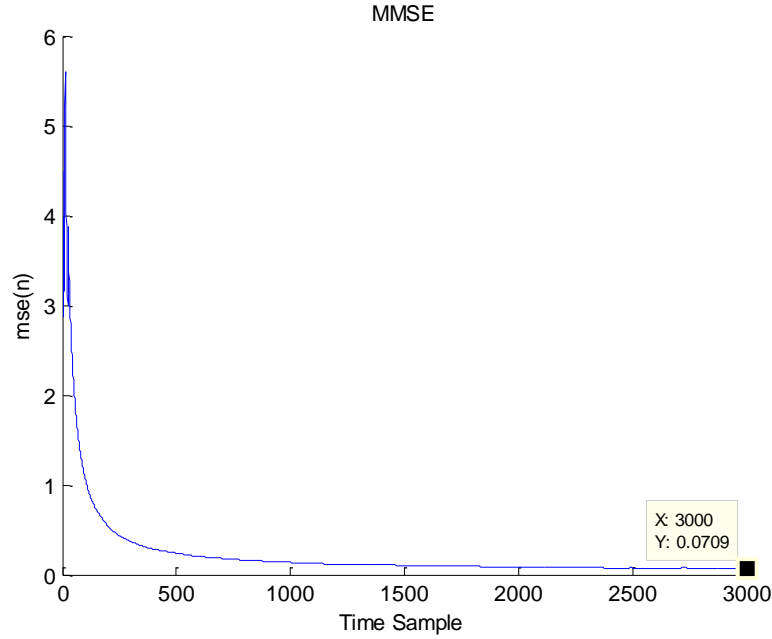


Figure 4.9 Mean-square symbol error of RLS algorithm.

From Figure 4.9, we can see that this algorithm works well when the second class of channel model is used. The MSE converges to 0.0709 at index sample  $n = 3000$ .

### 4.2.3 Experiment 2

In this experiment, the cyclic LMS algorithm, which is first presented in [11], is simulated with zero delay ( $d = 0$ ) using the first class of channel model (the raised-cosine two-ray multipath mobile radio) with  $L_g = L_h = 4$ . Figure 4.10 shows the equalized eye diagram, whereas Figure 4.11 depicts the mean-square symbol error for cyclic LMS algorithm across 3000 symbols. The additive noise is the same as last experiment. Trading off speed convergence with steady-state error, the performance

of cyclic LMS relies on the step size  $\mu$  which throughout this thesis is chosen to be 0.0025. For simulation, use equation (3.23).

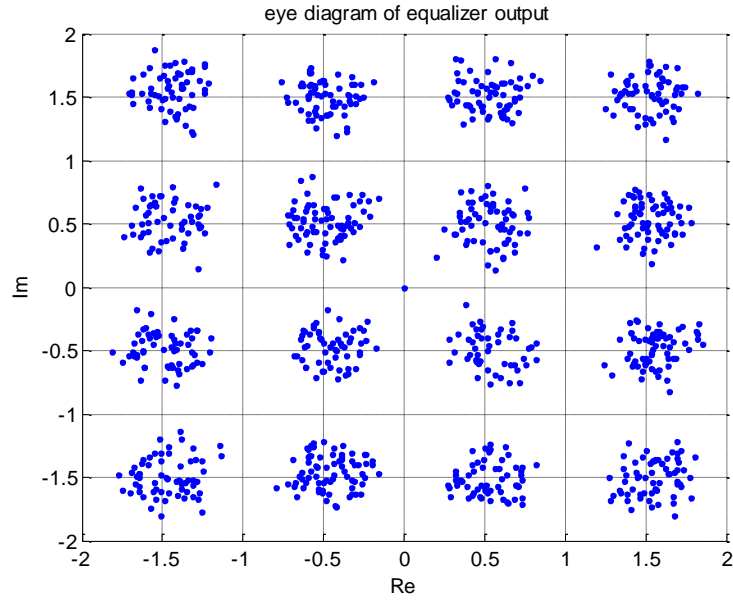


Figure 4.10 Eye diagram of equalizer output, using cyclic LMS with the raised-cosine channel.

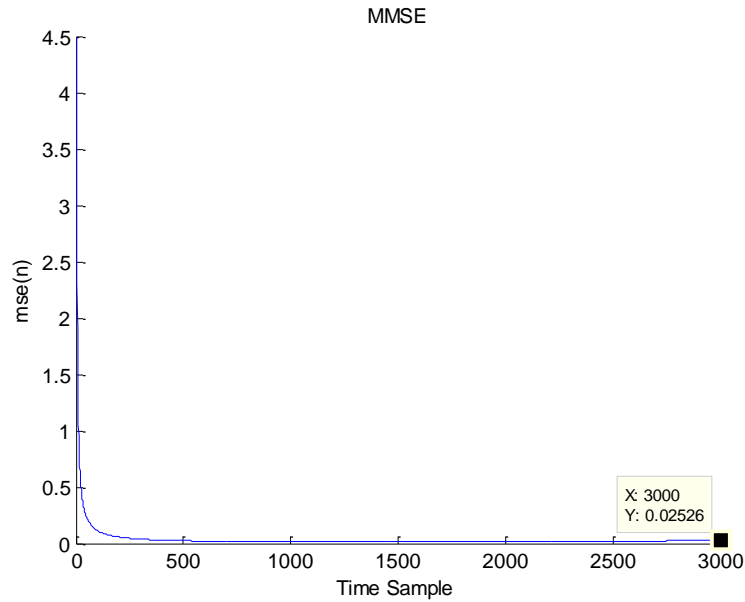


Figure 4.11 Mean-square symbol error of cyclic LMS.

From Figure 4.11, the performance of cyclic LMS is better than RLS algorithm since cyclic LMS has lower MSE and faster convergence. The MSE converges to 0.02526 at index sample  $n = 3000$ . However, the cyclic LMS doesn't work with the second class of channel model. To make it work, the conjugate calculation  $y_{Lg}^*(N)$  in (3.23) has to be removed. Otherwise, it won't work.

#### 4.2.4 Experiment 3a

In this experiment, The LMS algorithm is performed using the raised-cosine channel with zero delay ( $d = 0$ ). We still suppose the same assumption as in the experiment 2. Figure 4.12 shows the equalized constellation, while the mean-square symbol error is estimated for this algorithm across 3000 symbols as shown in Figure 4.13. For simulation, use equations (3.29) and (3.30).

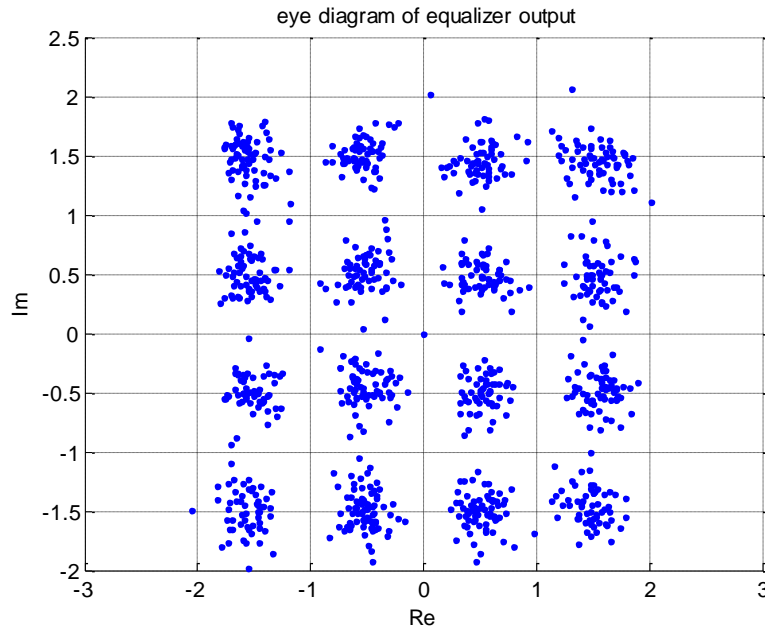


Figure 4.12 Equalized eye diagram, using LMS algorithm with the raised-cosine channel.

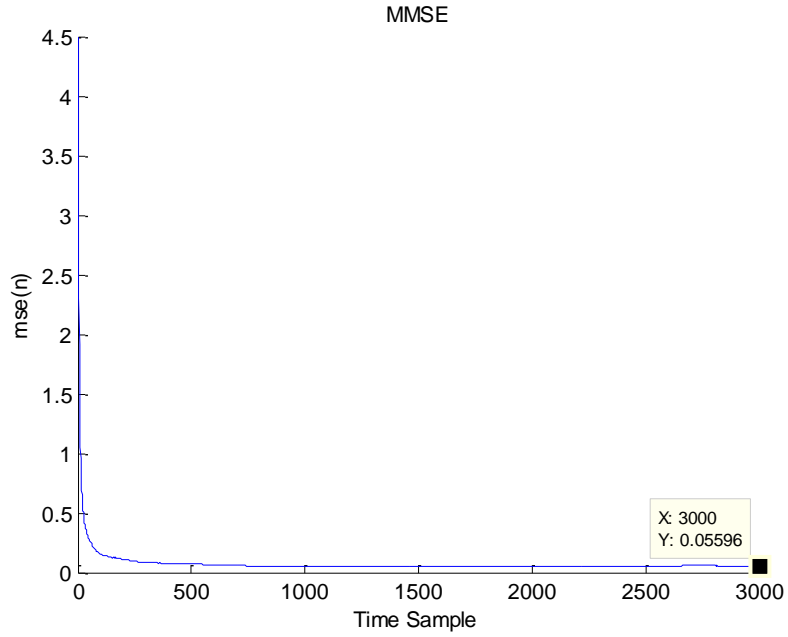


Figure 4.13 Mean-square symbol error of LMS algorithm.

As we see from Figure 4.13, the LMS method works well. The MSE converges to 0.05596 at index sample  $n = 3000$ .

#### 4.2.5 Experiment 3b

In this section, the second class of channel model is used to implement the LMS algorithm. Our assumptions are still the same as in previous section. Figure 4.14 shows the equalized eye diagram, whereas Figure 4.15 depicts the mean-square symbol error for LMS algorithm across 3000 symbols.

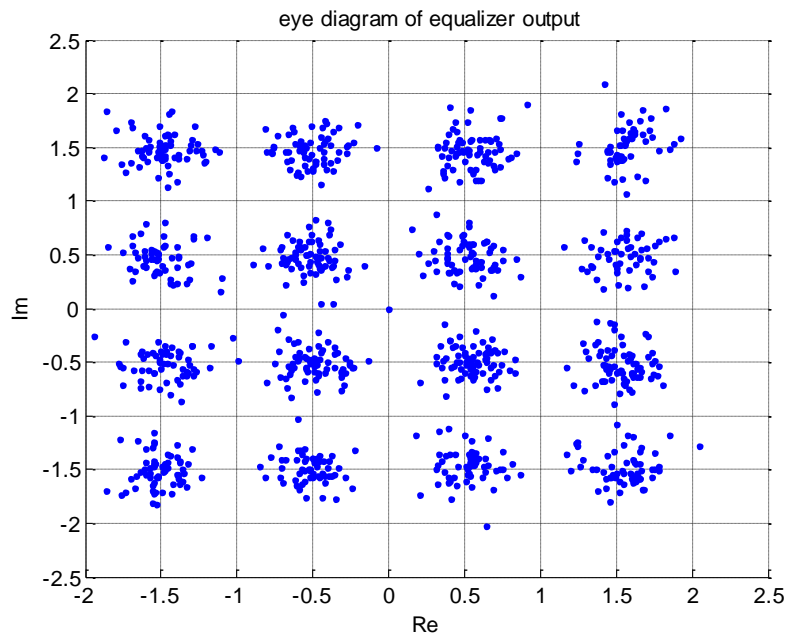


Figure 4.14 Eye diagram of equalizer output, using LMS algorithm with the second class of channel model.

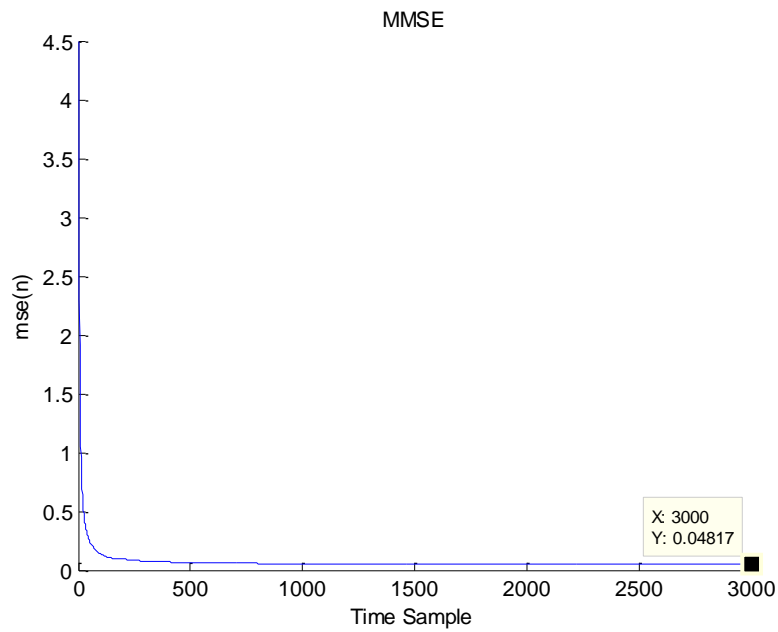


Figure 4.15 Mean-square symbol error of LMS algorithm.

From Figure 4.15, the performance of this experiment is better than experiment 3a since the MSE of LMS using the second class of channel model has lower value at 3000 (index sample). For more clarity, the MSE converges to 0.04817 at index sample  $n = 3000$ .

The comparison between RLS, cyclic LMS and LMS is accomplished through Figure 4.16 that shows the MMSE for the cyclic LMS, LMS and RLS. The channel used for this comparison is the raised-cosine two ray multipath mobile radio ( $P = 2$ ). The plot demonstrates that the cyclic LMS has better performance since it has the lowest MSE. The MSE of LMS is lower than the MSE line of the RLS at ( $n = 3000$ ).

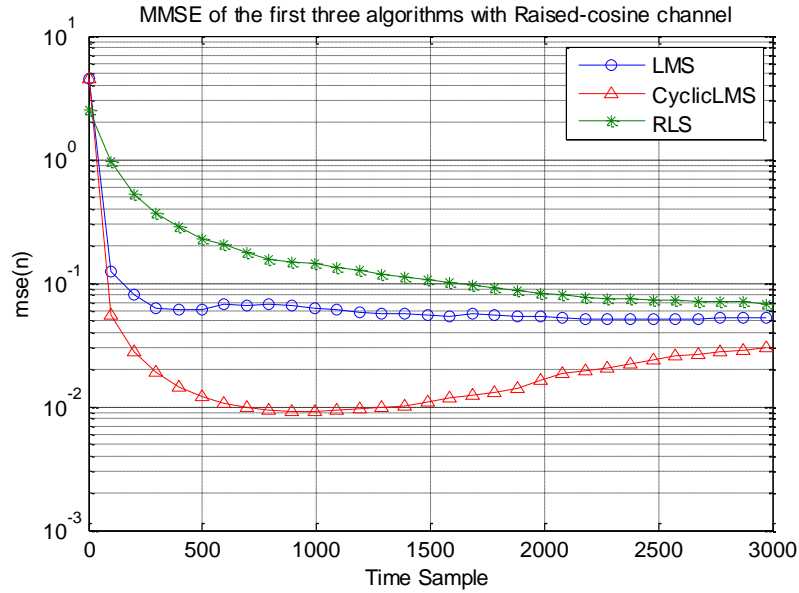


Figure 4.16 Mean-square symbol error, Comparison using raised-cosine channel.

The second comparison is also between cyclic LMS, LMS and RLS, but here the second class of channel model is used. We can see from figure (4.17) that the RLS has the best performance due to its MSE, which is lower than the MSE of both cyclic LMS and LMS. As I mentioned earlier that the cyclic LMS doesn't work with this channel class and it will not converge.

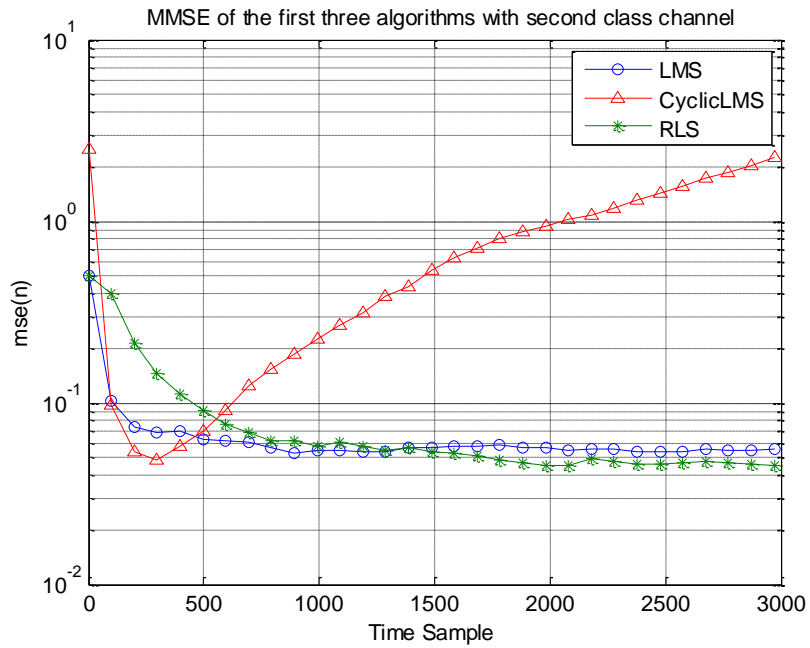


Figure 4.17 Mean-square symbol error, Comparison using second class of channel model.

#### 4.2.6 Experiment 4a

In this experiment, the unbiased blind adaptive using Gradient Projection (GP) technique is implemented. It is first presented in [10]. The channel used is the raised-cosine two-ray multipath mobile radio with  $L_g = L_h = 4$ . The small step size  $\alpha$  is chosen to be 0.002. The performance of linear prediction relies on the constraint value  $\gamma$  due to its impact on the MSE behavior. Throughout this thesis,  $\gamma$  is chosen to be 1.5. Figures 4.18 and 4.19 illustrate the behavior of this algorithm in a white noise situation. For simulation, use equations (3.31)–(3.34).

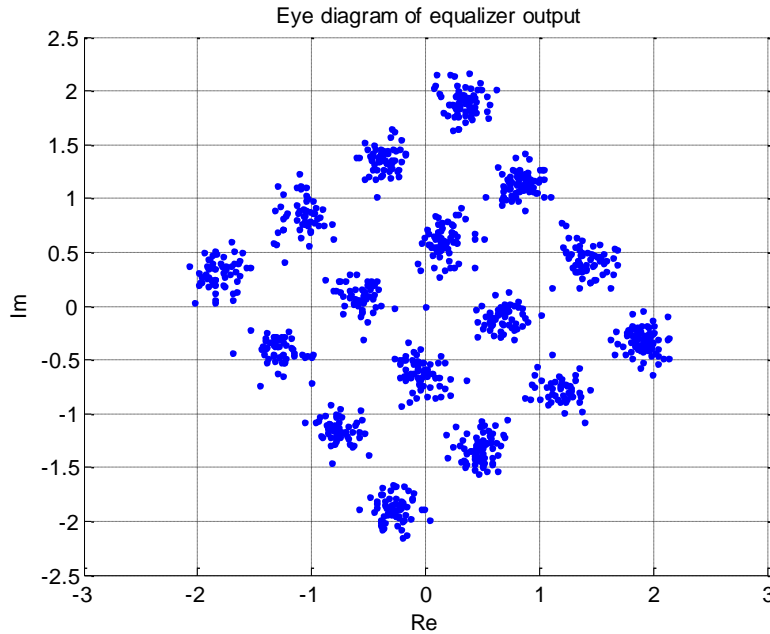


Figure 4.18 Eye diagram of equalizer output, using LP method with the raised-cosine channel.

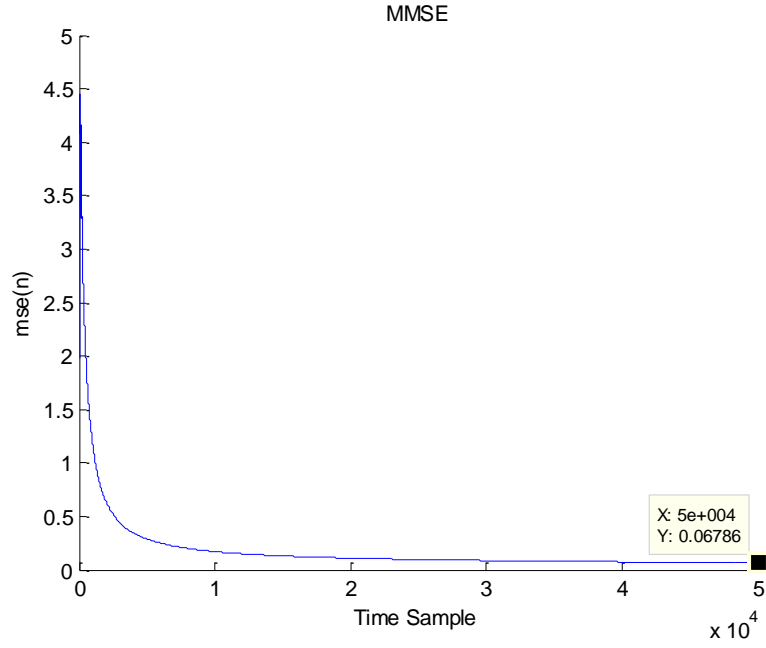


Figure 4.19 Mean-square symbol error of LP method.

From Figure 4.18 and 4.19, we see that this algorithm works well to equalize the received noisy signal. The MSE converges to 0.06786 at index sample  $n = 50000$ . The problem with this algorithm is it has slow convergence. The amount of rotation and magnification in the eye diagram (see Figure 4.18) is a function of  $h_0(0) = (0.52 - j0.72)$  which is the leading coefficient in  $\mathbf{h}_0$ . The angle of rotation is  $54.16^\circ$ , and the magnification is  $|h_0(0)| = 0.88$ .

#### 4.2.7 Experiment 4b

The second class of channel model is simulated in this experiment with using the same method as in experiment 4a. Our assumptions are still the same. Figure 4.20 shows the equalized eye diagram, while Figure 4.21 depicts the mean-square symbol error across 50000 symbols.

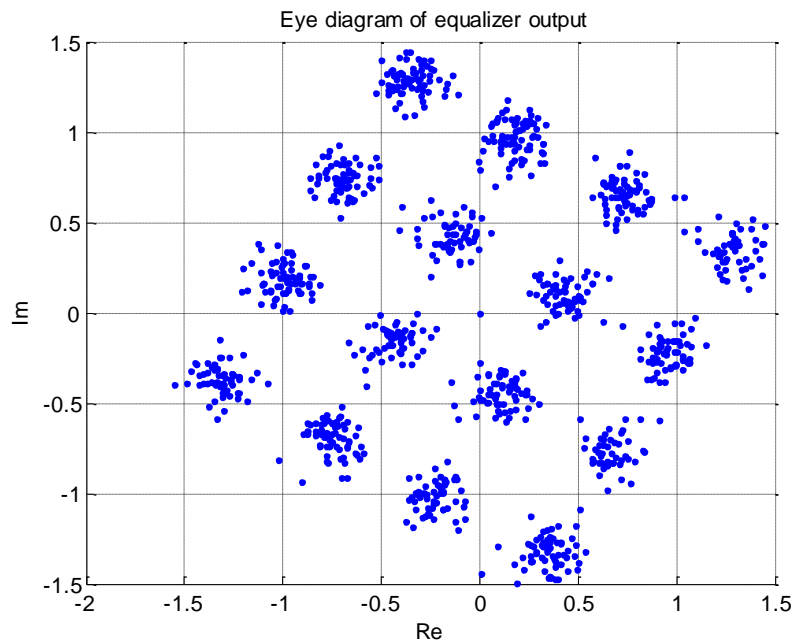


Figure 4.20 Eye diagram of equalizer output, using LP algorithm with the second class of channel model.

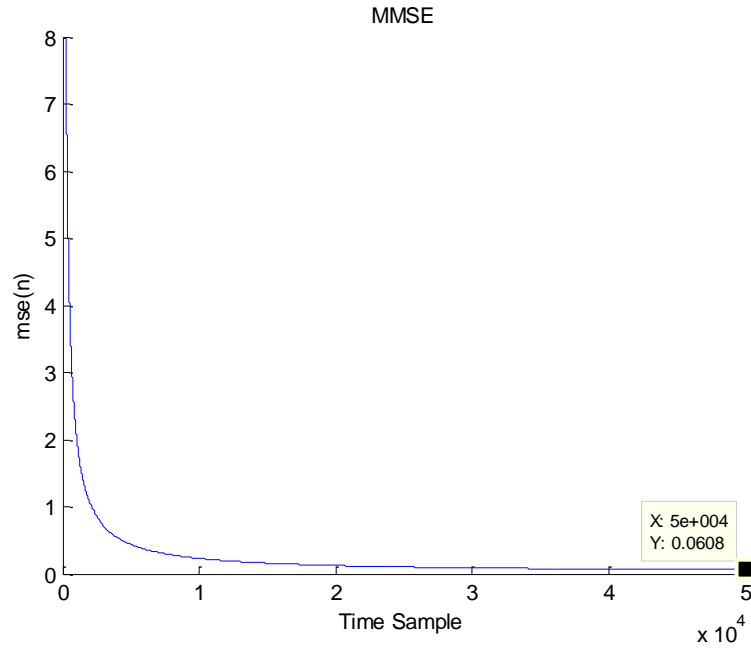


Figure 4.21 Mean-square symbol error of LP algorithm.

The algorithm works very well as we see from Figure 4.21 and the MSE converges to 0.0608 at time sample (50000). The performance is slightly better than that in experiment 4a. However, we are still facing the slow convergence problem. The leading parameter  $h_0(0) = (0.5498 - j0.3174)$ . The angle of rotation is  $30^\circ$ , and the magnification is  $|h_0(0)| = 0.635$ .

### 4.2.8 Experiment 5a

In this section, we use a symbol sequence that is assumed to be uncorrelated and generated from a 16- QAM constellation with -1.5, -0.5, 0.5 and 1.5 levels. The RELS algorithm, which is first presented in [22], is simulated using the following (third class) IIR channel model

$$A(q^{-1}) = 1 - 0.8q^{-1} + 0.41q^{-2}. \quad (4.9)$$

$$F(q^{-1}) = 1 + (0.5 - 0.6i)q^{-1}. \quad (4.10)$$

$$B(q^{-1}) = 0.5498 - 0.3174i + (0.4342 - 0.4596i)q^{-1} + (0.0131 - 0.0919i)q^{-2} + (-0.0275 + 0.1592i)q^{-3}. \quad (4.11)$$

$$C(q^{-1}) = 0.0414 - 0.0717i + (0.7168 - 0.3407i)q^{-1} + (0.0745 - 0.3636i)q^{-2} + (0.0685 - 0.1861i)q^{-3}. \quad (4.12)$$

Our assumptions with respect to additive noise are still the same. Figure 4.22 shows the received symbols  $x_1(i)$ , while Figure 4.23 shows the equalized symbols eye diagram. As performance measures, the mean-square symbol error for RELS algorithm across 3000 symbols is estimated as shown in Figure 4.24 using the following equation

$$mse(n) = \frac{1}{n} \sum_{i=0}^n |x_1(i+1) - \hat{y}(i+1) - b_0 w(i+1)|^2. \quad (4.13)$$

For simulation, use equation (3.49)-(3.53).

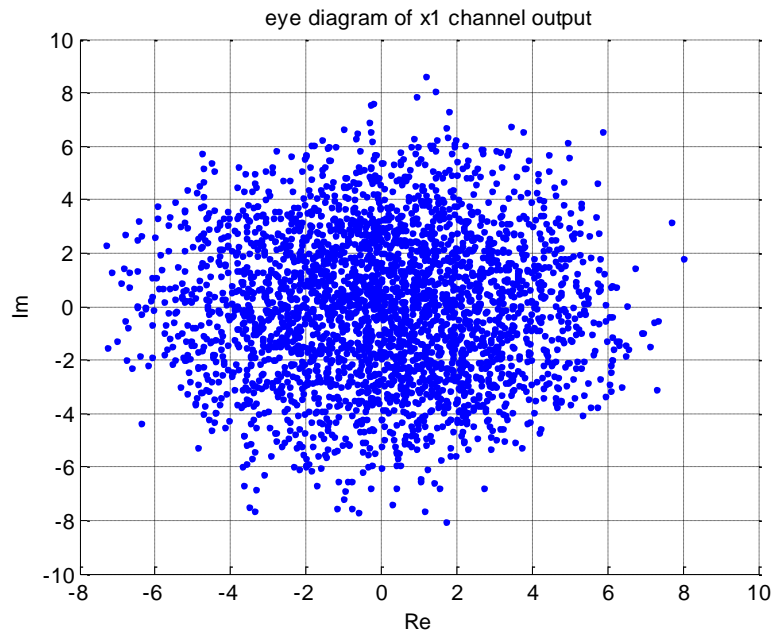


Figure 4.22 Eye diagram of received signal for 16 QAM modulation.

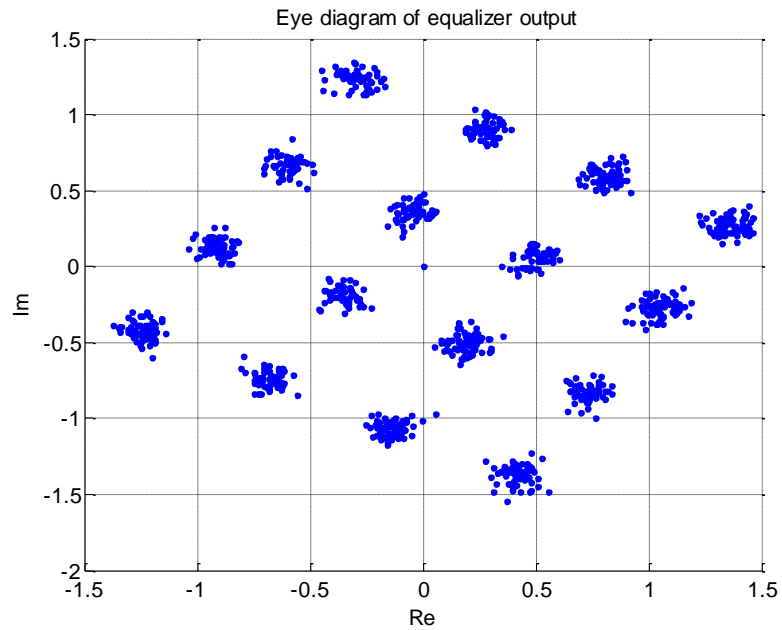


Figure 4.23 Eye diagram of equalizer output, using RELS algorithm with the third class of channel model (IIR).

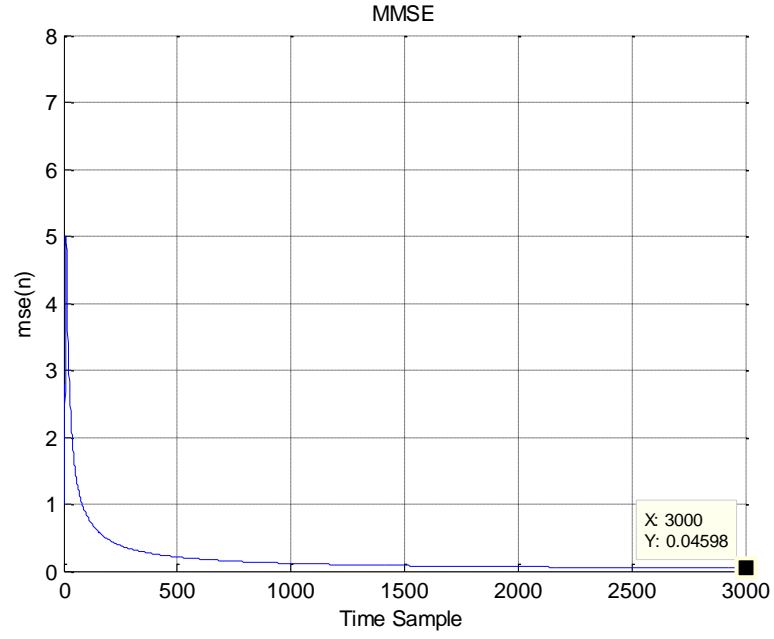


Figure 4.24 Mean square symbol error of RELS algorithm.

#### 4.2.9 Experiment 5b

In this section, we run the algorithm with the presence of the modeling error in the channel dynamics, and we use the same polynomials as in Experiment 5a,

$$\begin{aligned}
 x_1(i) &= \frac{B(q^{-1})F(q^{-1})}{A(q^{-1})}w(i) + v_1(i) + \delta_1(i), \\
 x_2(i) &= \frac{C(q^{-1})F(q^{-1})}{A(q^{-1})}w(i) + v_2(i) + \delta_2(i).
 \end{aligned} \tag{4.14}$$

where  $v_1(i)$  and  $v_2(i)$  are white noise with zero mean and variance=0.14. It is important to mention that  $v_k(i)$ ,  $k = 1, 2$ , and  $w(i)$  are independent sequences. Let  $\delta_k(i)$ ,  $k = 1, 2$ , are modeling errors given by

$$\delta_1(i) = \frac{\delta}{1 - 0.5q^{-1}} w(i) \quad \text{and} \quad \delta_2(i) = \frac{\delta}{1 + 0.7q^{-1}} w(i), \quad (4.15)$$

where  $\delta$  is a parameter defining the size of the channel modeling error. Figures 4.25 and 4.26 illustrate the scatter plot of the equalized symbols and sample mean-square error, respectively, with setting  $\delta = 0.1$  in (4.15).

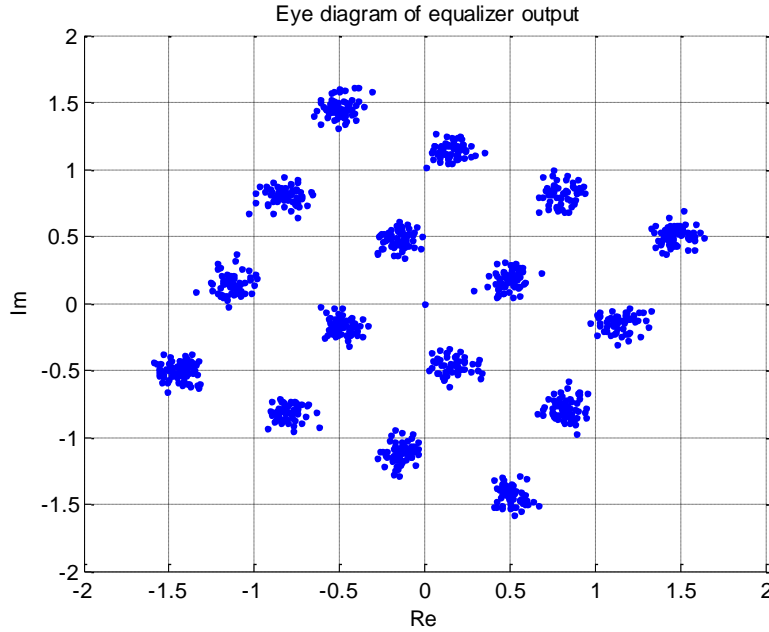


Figure 4.25 Scatter plot of equalized symbols, using RELS algorithm with the presence of modeling error using (IIR) channel.

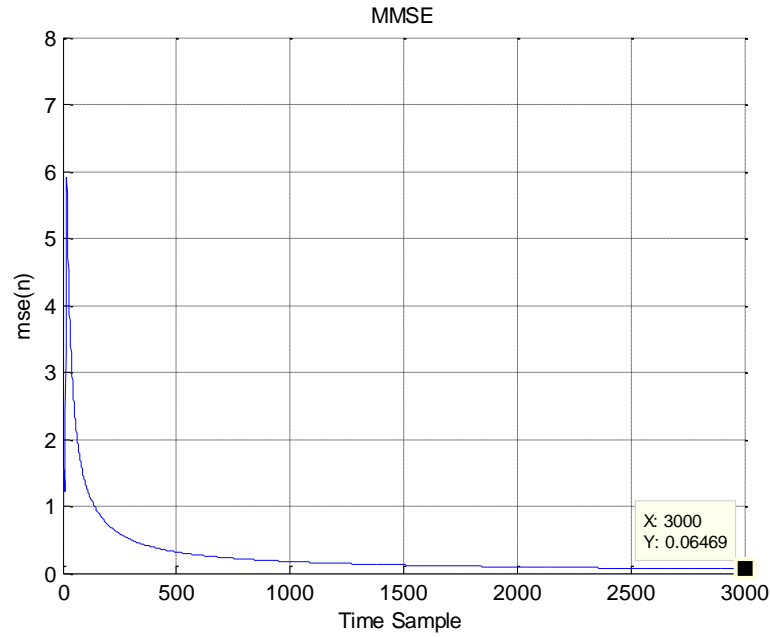


Figure 4.26 Sample mean square error of RELS algorithm.

This algorithm shows a very good performance of equalizing the received signal with and without presence of noise and modeling error as illustrated in both Figures 4.24 and 4.26. The MSE converges to 0.04598 at index sample  $n = 3000$  in experiment 5a, whereas the MSE of experiment 5b converges to 0.06469 at the same index sample. Therefore, it is clear that the algorithm provides a degree of robustness with respect to receiver noise and modeling error [22].

The comparison between all of these algorithms is done with using the second class of channel model. Figure 4.27 demonstrates that the performance of RELS algorithm is the best since its MSE has the lowest value at the time sample ( $n = 3000$ ).

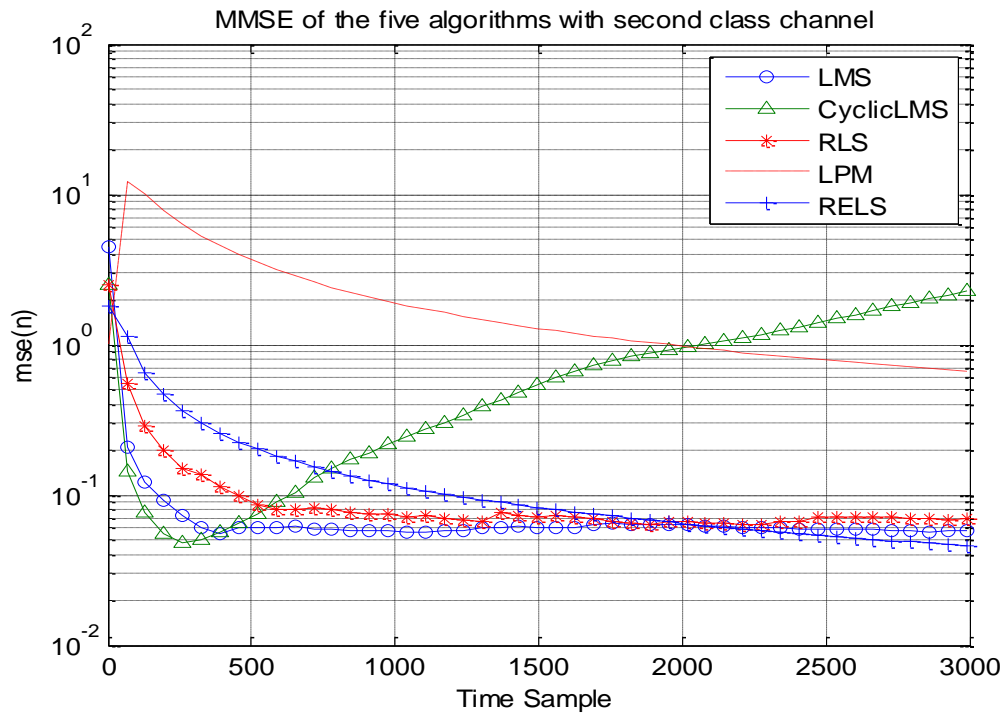


Figure 4.27 Mean-square symbol error, Comparison for those five algorithms with the second class of channel model.

## **CHAPTER V**

### **CONCLUSION**

This thesis has proved how adaptive blind algorithms (RLS, cyclic LMS, LMS, LP and RELS) can equalize the wireless communication channels through removing inter-symbol-interference (ISI). These techniques have proven to be quite effective and powerful to combat ISI effect. ISI is mainly generated in dispersive channels such as Radio and Mobile wireless channels. In a particular case, the mobile cellular communication (multipath propagation of the transmitted signal) suffers from severe ISI. Therefore, an adaptive filter as an equalizer can be placed at the receiver to compensate or equalize the dispersion occurred during transmission. This filter or the equalizer is a device positioned at the receiver to alleviate the effect of ISI and thus the transmitted symbol sequence can be recovered.

Channel equalization methods used in this thesis rely only on the statistical behavior of the received signals (Second order Statistics) in order to estimate the transmitted sequence without requiring the knowledge of the channel characteristics. The transmission environments used were a raised-cosine SIMO channel model realized by fractionally sampled (FS) FIR filter, SIMO channel model with constant coefficients over period realized by (FS) FIR filter and SIMO channel model realized by (FS) IIR filter. The latest channel model was performed with and without modeling error.

It has been shown that the algorithms used in this thesis perform very well, and they are very efficient and robust with respect to the channel distortions through examining their mean square symbol error (MSE) performance via computer simulations. Also, it is shown that the RELS algorithm has an advantage over the rest of algorithms since it has the fastest MSE convergence.

For future research, our system might be extended to MIMO channel model case, and we should study and examine our techniques performance. Also, we may investigate the capability of adaptive blind channel equalization algorithms with using time-varying transmission channel and see which one provides computationally efficient implementations with and without presence of noise.

## REFERENCES

- [1] K. Abed Meraim, E. Moulines and P. Loubaton, "Prediction error methods for second-order blind identification," *IEEE Trans. Signal Processing*, vol. 45, pp. 694-705, Mar. 1997.
- [2] K. Abed Meraim *et al.*, "Prediction error methods for time-domain blind identification of multichannel FIR filters," in *Proc. Int. Conf. Acoust., Speech, Signal Processing*, vol. 3, Detroit, MI, 1995, pp. 1968-1971.
- [3] E. W. Bai and M. Fu, "Blind system identification and channel equalization of IIR system without statistical information," *IEEE Trans. Signal Processing*, vol. 47, pp. 1910-1920, July 1999.
- [4] A. Cichocki and S. Amari, *Adaptive Blind Signal and Image Processing: Learning Algorithms and Applications*, Chichester: John Wiley & Sons, 2002.
- [5] P. Comon and M. Rajih, "Blind identification of under-determined mixtures based on the characteristics function," *Signal Proc.*, vol. 86, pp. 2271-2281, September 2006.
- [6] H. Cox, R. Zeskind and M. Own, "Robust adaptive beamforming," *IEEE Trans. Acoust., Speech, Signal Processing*, vol. ASSP-35, Oct. 1987.
- [7] Z. Ding, *Adaptive Filters for Blind Equalization*, *CRC Press LLC*, 1999.
- [8] Z. Ding and Y. Li, "On channel identification based on second-order cyclic spectra," *IEEE Trans. Signal Processing*, vol. 42, pp. 1260-1264, May 1994.
- [9] P. S. R. Diniz, *Adaptive Filtering Algorithms and Practical Implementation*, 3<sup>rd</sup> ed. New York, NY: Springer Science & Business Media, LLC, 2008.

- [10] D. Gesbert and P. Duhamel, "Unbiased blind adaptive channel identification and equalization," *IEEE Trans. Signal Processing*, vol. 48, pp. 148-158, Jan. 2000.
- [11] G. Giannakis and S. Halford, "Blind fractionally spaced equalization of noisy FIR Channels: Direct and adaptive solutions," *IEEE Trans. Signal Processing*, vol. 45, pp. 2277-2292, Sept. 1997.
- [12] O. V. Goryachkin and E. I. Erina, "Given correlation manifolds and their application in blind channel identification," *The open Statistics and Probability Journal*, 2009, 1, 55-64.
- [13] S. Haykin, *Adaptive Filter Theory*, 2<sup>nd</sup> ed. Englewood Cliffs, NJ: Prentice-Hall, 1991.
- [14] S. Haykin, "Blind Deconvolution," S. Haykin Ed. *Adaptive Filter Theory*, NJ, Prentice-Hall, Englewood Cliffs, 1991.
- [15] R. A. Horn and C. R. Johnson, *Matrix Analysis*, New York, NY: Cambridge Press, 1985.
- [16] C. Johnson, P. Schniter, T. Endres, J. Behm, D. Brown and R. Cases, "Blind equalization using the constant modulus criterion: A Review," *Processing of the IEEE*, vol. 86, pp. 1927-1950, Oct. 1998.
- [17] J. Lebrun and P. Comon, "Blind algebraic identification of communication channels: symbolic solution algorithms," *Appl. Ageber. Eng. Commun. Comput.*, vol. 17, pp. 471-485, November 2006.
- [18] E. Moulines, P. Duhamel, J. F. Cardoso and S. Mayrargue, "Subspace methods for the blind identification of multichannel FIR filters," *IEEE Trans. Signal Processing*, vol. 43, pp. 516-525, Feb. 1995.

- [19] B. Porat and B. Friedlander, "Blind equalization of digital communication channels using higher-order moments," *IEEE Trans. Signal Processing*, vol. 39, pp. 522-526, Feb. 1991.
- [20] J. Proakis and M. Salehi, *Digital Communications*, New York: McGraw-Hill, 5<sup>th</sup> ed., 2008.
- [21] M. Radenkovic, T. Bose and Z. Zhang, "Self-tuning blind identification and equalization of IIR channels," *EURASIP Journal on Applied Signal Processing* 2003:9, 930-937.
- [22] M. Radenkovic, T. Bose, "A recursive blind adaptive equalizer for IIR channels with common zeros," *Circuit Syst. Signal Process*, 28, 467-486, 2009.
- [23] O. Shalvi and E. Weinstein, "New criteria for blind deconvolution of nonminimum phase systems (channels)," *IEEE Trans. Inform. Theory*, vol. 36, pp. 312-321, Mar. 1990.
- [24] D. T. M. Slock, "Blind fractionally-spaced equalization, perfect-reconstruction filter banks and multichannel linear prediction," in *Proc. Int. Conf. Acoust., Speech, Signal Processing*, vol. IV, Adelaide, Australia, 1994, pp. 585-588.
- [25] G. H. Stuck, "Adaptive blind equalization with applications in communication systems," *MS Thesis*, University of Colorado at Denver, April 2002.
- [26] L. Tong, G. Xu and T. Kailath, "Blind identification and equalization based on second-order statistics: A time domain approach," *IEEE Trans. Inform. Theory*, vol. 40, pp. 340-349, Mar. 1994.
- [27] L. Tong, G. Xu, B. Hassibi and T. Kailath, "Blind channel identification based on second-order statistics: A frequency domain approach," *IEEE Trans. Inform. Theory*, vol. 41, pp. 329-334, Jan. 1995.
- [28] L. Tong and S. Perreau, "Multichannel blind identification: From subspace to maximum likelihood methods," *Proc. IEEE*, vol. 86, pp. 1951-1968, 1998.

- [29] J. T. Tugnait, L. Tong and Z. Ding, "Single-user channel estimation and equalization," *IEEE Signal Proc. Mag.*, vol. 12, pp. 17-28, 2000.